Published in final edited form as:
Int J Hyperthermia. 2011 ; 27(4): 320–343. doi:10.3109/02656736.2010.534527.

Thresholds for thermal damage to normal tissues: An update

Pavel S. Yarmolenko[1,2], **Eui Jung Moon**[3,4], **Chelsea Landon**[3,5], **Ashley Manzoor**[5,6], **Daryl W. Hochman**[7], **Benjamin L. Viglianti**[8], and **Mark W. Dewhirst**[3,5]

[1]Department of Biomedical Engineering, Duke University, Durham, North Carolina [2]Center for Interventional Oncology, Radiology and Imaging Sciences, Clinical Center, National Institutes of Health, Bethesda, Maryland [3]Department of Pathology, Duke University, Durham, North Carolina [4]Department of Radiation Oncology, Stanford University, Stanford, California [5]Department of Radiation Oncology, Duke University, Durham, North Carolina [6]Medical Physics Program, Duke University, Durham, North Carolina [7]Department of Surgery, Duke University, Durham, North Carolina [8]Department of Radiology, University of Michigan, Ann Arbor, Michigan, USA

Abstract

The purpose of this review is to summarise a literature survey on thermal thresholds for tissue damage. This review covers published literature for the consecutive years from 2002–2009. The first review on this subject was published in 2003. It included an extensive discussion of how to use thermal dosimetric principles to normalise all time-temperature data histories to a common format. This review utilises those same principles to address sensitivity of a variety of tissues, but with particular emphasis on brain and testis. The review includes new data on tissues that were not included in the original review. Several important observations have come from this review. First, a large proportion of the papers examined for this review were discarded because time–temperature history at the site of thermal damage assessment was not recorded. It is strongly recommended that future research on this subject include such data. Second, very little data is available examining chronic consequences of thermal exposure. On a related point, the time of assessment of damage after exposure is critically important for assessing whether damage is transient or permanent. Additionally, virtually no data are available for repeated thermal exposures which may occur in certain recreational or occupational activities. For purposes of regulatory guidelines, both acute and lasting effects of thermal damage should be considered.

Keywords

thermal damage threshold; thermal dosimetry; normal tissue damage; thermal injury

Introduction

The objective of this review is to compile and analyse thermal tissue damage data that has become available since the last review on this subject was published in *International Journal of Hyperthermia* in 2003 [1]. This work concentrates on identifying thresholds for thermal damage, the dependence of severity of damage on thermal dose, and permanence of damage in various tissues. Complex organs such as the brain also experience a myriad of functional changes, some of which this review also addresses. The previous review on the subject

Correspondence: Mark W. Dewhirst, Box 3455 DUMC, Room 201 MSRB, Research Drive, Durham, NC, 27710, USA. Tel: (919) 684-4180. Fax: (919) 684-8718. mark.dewhirst@duke.edu.

stressed the importance of cumulative thermal dose as a determinant of tissue thermal damage. Cumulative equivalent minutes at 43°C (CEM_{43}) is the accepted metric for thermal dose assessment that correlates well with thermal damage in a variety of tissues [1]; this work concentrates on data for which CEM_{43} could be calculated. The calculation of CEM_{43} involves knowledge of thermal history:

$$CEM_{43}=\Delta t R^{(43-T)} \quad (1)$$

where Δt signifies summation over the length of exposure, T is the average temperature during time interval t, and R is a constant equal to 0.25 for $T<43°C$ and 0.5 for $T>43°C$ [1, 2]. Since the values of CEM_{43} have been found to correlate with severity of thermal damage, this review was primarily limited to published data that include analysis of tissue damage (severity and threshold) at the locations where thermal history is available.

Beginning with the year 2002, 463 papers were identified, using an extensive list of keywords (Table I). In addition to keyword searches, we also performed recursive searches of papers that cited the 2003 review. The majority of the papers were not included in the analysis of thermal damage due to a number of factors: (1) incomplete thermal data (88 publications), these are papers where temperature was not measured at the site of damage assessment, or not measured at all; (2) reviews without original data (63 publications) were the second most-excluded type of article; (3) many publications involved heating with lasers to very high thermal doses that result in complete tissue destruction well before thermal dose could be estimated (56 publications), or they did not quantify damage at the site where temperature was measured (43 publications); (4) modelling papers without original data were excluded (35 publications), as were (5) papers where assessment of thermal damage was done on excised tissues (26 publications). These were excluded due to a large variability in handling of *ex vivo* samples and other confounding factors, such as tissue viability and lack of perfusion in *ex vivo* heating experiments, which could influence thermal damage [3].

An abundance of recent brain and testicle thermal damage data has resulted in a major concentration on these tissues. The focus on these two tissues is useful to bring out principles that are applicable to other tissues as well. A summary of thermal damage data for other tissues is provided.

Our findings are complimentary to the earlier review. Table II shows the summary data from the earlier review along with findings reviewed herein. The new data do not call for a revision of thresholds for thermal damage of tissues that were included in the original review. However, much of the new data (bold in the table) is concentrated at the extreme low and high ranges of CEM_{43}, while little new data were found in the intermediate range of CEM_{43}=21–40 min. More data in the intermediate dose range, as well as more data on chronic, rather than acute effects of heat would enrich knowledge of this subject. It is imperative that temperature is measured at the site of induced damage in future studies that address thermal damage thresholds.

The effects of heat differed between tissues within each species, as well as between species. It is important to note that the severity of damage was highly dependent upon when the assessment was made. This report will review the data available and make recommendations about the needs of future research in this area.

Discussion of specific organs and organ systems

Nervous system

Overview—A wide range of endpoints have been reported since the previous review. Here we report data concerning vascular changes, direct damage, and functional and metabolic effects on the nervous system due to heat stress. Exposure temperatures reached as high as 48°C, resulting in body temperatures up to 43°C. The majority of the following studies used whole body hyperthermia followed by acute (1–30 days) assessment, so the permanence/reversibility of the following effects is unknown. While damage threshold data is available for several species, the overwhelming majority of the studies were performed with rats. Thermal damage endpoints in these studies can be classified into three categories: (1) vascular effects, (2) direct damage, and (3) functional effects.

Vascular effects

Blood–brain barrier (BBB) permeability—Kiyatkin et al. [4], Sharma [5], and Noor et al. [6] assessed regional BBB permeability after whole body hyperthermia treatment (Figure 1). Two of the three studies showed that heating increased BBB permeability in the range of thermal doses examined. Kiyatkin et al. anaesthetised adult (~460 g) male Long-Evans rats with pentobarbital and treated them with whole body hyperthermia via a warming pad for 75 min (peak temperature range 38.6°–41.8°C). Sharma et al. treated male albino Wistar rats (9–10 weeks old) with whole body hyperthermia using a biological oxygen demand incubator (38°C for 30 min, 1, 2, 3 and 4 h (average core temperature 41°C)) without anaesthesia. Noor et al. assessed BBB permeability after heating for 180 min at either 38°C or 39°C (CEM_{43} range: 0.1–0.7 min) using a warming pad. Since 38°–39°C is within the normal body temperature range for rats, it is not surprising that no change in permeability was observed after treatment.

BBB Permeability was assessed 24 h after heating through detection of extravasated Evans blue dye by Noor et al., immediately after heating with cell-bound albumin (Kiyatkin et al.), or a combination of Evans blue-labeled albumin and ^{131}Iodine (Sharma et al.). These permeability assessments were made at similar CEM_{43}, both in the Noor et al. and in Kiyatkin et al. studies (0.1–0.7 and 0.03–0.7 min, respectively). A significant increase was observed by Kiyatkin et al. in all regions of interest (Figure 1A). Rats in the Kiyatkin et al. study (Figure 1A) also underwent significantly higher CEM_{43} than the other studies (Figure 1B). The thalamus, hippocampus, and piriform areas of the brain were relatively more sensitive to the effects of heating. In the Sharma et al. study, assessments were made 4 h following heating to CEM_{43}=1.3 min (Figure 1B). Rat cingulate and temporal brain regions experienced the greatest increases in BBB permeability due to heat (18- and 9-fold increases, respectively). While brain region sensitivities vary between the studies, heat treatment increases BBB permeability across all brain regions examined, and as shown in the Kiyatkin et al. study, permeability increases with higher CEM_{43}, in the range of CEM_{43} examined. Sensitivity differences may be due to the different heat regimes (longer exposure and lower temperature compared to shorter exposure and higher temperature), anaesthesia used, timing, rat strain, or a combination.

Oedema—Kiyatkin et al. [4] and Sharma [5] also assessed oedema by measuring water content in the brain after whole body heating. Both studies observed an increase in oedema, although the Kiyatkin et al. study reported less oedema (3.5–4.1% increase) than the Sharma study (4–7% increase), even though rats in the Kiyatkin et al. study were exposed to higher CEM_{43}. The difference cannot be evaluated statistically, and the higher oedema observed by Sharma et al. may be a result of the duration of exposure rather than exposure intensity. As

stated previously, such differences may also arise from the difference in heating methods, anaesthesia, rat strain, or a combination of these discrepancies between studies.

Cerebral blood flow—Several papers assessed the effect of whole body heating on cerebral blood flow for several different species, including rats, rabbits, and humans (Figure 2). Two of the papers showed an increase in blood flow (Cremer et al. [7] in humans and Sharma et al. [5] in rats), while the other two papers showed a decrease (Chou et al. [8] in rats and Mustafa et al. [9] in rabbits). Although the data seem to contradict each other, animals were heated differently in each study, with greatly varying CEM_{43}.

Chou et al. treated adult male Sprague-Dawley rats anaesthetised with intraperitoneal urethane with whole body heating via a water blanket for 20–70 min set at 42°C (body temperature range 37.5–41.5°C). Cerebral blood flow was assessed with a laser Doppler flow meter. Sharma et al. treated animals as described (see BBB permeability above) and assessed cerebral blood flow with microspheres labelled with iodine.

Humans anaesthetised with an infusion pump of propofol-fentanyl-rocuronium have been assessed in a heating study [7]. Humans were treated with whole body heating via an extracorporeal heater-cooler device with a bifemoral venovenous circuit for 90 min (body temperature ≈41.8°C). Cerebral blood flow was measured with transcranial pulsed Doppler ultrasonography. It should be noted that the humans studied were diagnosed with chronic hepatitis C and ranged in age from 18 to 65 years.

Mustafa et al. examined New Zealand white rabbit (10 weeks old) cerebral blood flow by monitoring injected 99mTc-HMPAO with a Gamma camera after treating with whole body hyperthermia in a temperature-controlled chamber (45°C) for 60 min [9]. Body temperature was maintained at 43°C, and it should be noted that this is an extremely high temperature for mammals and not likely a survivable thermal exposure. Rabbits were anaesthetised with intravenous sodium pentobarbital prior to treatment.

In summary, not enough data exists to generalise the effects of heat on cerebral blood flow. The two studies on rats contradict each other, with Sharma et al. observing an increase whereas Chou et al. saw a decrease. These observations were made following much lower thermal doses than the data available for humans and rabbits, where heat also affected cerebral blood flow in divergent directions (Figure 2). Regardless of the technique used and the direction of the change, all studies reported significant changes in cerebral blood flow after whole body hyperthermia treatment.

Direct damage

Cell death—Khan et al. [10] assessed cell death in several portions of the adult rat cerebellum (granule cell layer, molecular layer, and deep white matter) as well as in rat pup (P7) cerebellum. Male Wistar rats (30 days old) and P7 rat pups were treated with whole body heating via a dry air incubator (42°C) for 60 min after reaching the set temperature (body temperature 41.3°C for 60 min) without anaesthesia. TUNEL was used to assess cell death at multiple endpoints after heat exposure 2.5, 5, 10, 15, 24 h for the adults and 5, 10, 15, 24 h for the pups (Figure 3A). At the same CEM_{43} (5.9 min), pups seemed much more sensitive to the heat stress showing induced cell death 10 h after treatment, but by 24 h levels reverted back to baseline level of cell death, suggesting a transient effect. The specific layers of the cerebellum in adult rats were more resistant to the stress. In Belay et al. [11] adult male Wistar rats (45 days old) were treated with whole body hyperthermia via a dry-air incubator (43°C) for 1 h once core temperature reached 42°C. Rats were not anaesthetised during hyperthermia treatment. Cell death was assessed 10 h after heat treatment in several brain regions with TUNEL assay. Sensitivity differences were present among the three

regions assessed; pia mater was the most sensitive followed by corpus callsum and fimbria in order of decreasing sensitivity (Figure 3B).

Central nervous system damage (cell abnormalities, damage, and distortion)—Kiyatkin et al. [4] treated male Long-Evans rats as described above in 'BBB permeability' and assessed cellular abnormalities by hematoxylin and eosin (H&E) staining with the following criteria (abnormal cells having one or more of the following characteristics): altered (swollen or shrunken) shape, distorted nucleus, chromatolysis, dark neurons and eccentric nucleolus. Various portions of the brain all had similar sensitivities with increasing damage plotted against increasing CEM_{43} except for the thalamus (Supplementary Figure 1A). The thalamus was extremely sensitive relative to the other brain regions. While the thalamus reached 100% of the maximum cellular abnormalities noted at the highest CEM_{43} (close to 2 min), all other brain regions reached only 50%. Damage in other brain regions increased consistently with increasing CEM_{43}. Sharma [5] treated male albino Wistar rats as described in BBB permeability above. In that study, central nervous system (CNS) damage/distortion was measured by light/electron microscopy, using the following scoring system: 0=absent, 1=mild, 2=moderate, and 4=severe. The scoring system reflects increases in nerve and glial cell reaction, dark and distorted nerve cells, loss of nerve cells, sponginess, oedema, and loss of myelin. Increasing damage/distortion was observed with increasing CEM_{43} (Supplementary Figure 1B). Maximum damage/distortion was observed at a CEM_{43}=1.3 min.

As observed with the BBB permeability, cellular damage seems to be higher for longer, lower temperature exposures than with shorter, higher temperature exposures. The long, lower temperature exposures that showed relatively high CNS damage were similar in duration and peak temperature to a fever, and therefore these data may contribute to the understanding of effects of fever on CNS. The lower levels of damage following shorter, higher temperature exposures may be useful in design of focused ultrasound heating treatments.

Functional effects

Breathing rate during heating—Schuchmann et al. [12] assessed the breathing rates of Wistar rat pups (in P8–P11 and P22–P23 stages of development). Pups underwent whole body hyperthermia via a 48°C chamber for 55 min without anaesthesia. Peak rectal temperature for the P22–23 and the P8–11 rats was 44.2°C and 43.6°C, respectively. As depicted in Supplementary Figure 2, breathing rate increased at very low CEM_{43} values. The younger pups (P8–P11) peaked and plateaued at a breathing higher rate than the older (P22–P23) pups (approximately 55–60% increase compared to 20–25% increase, respectively). The peak and plateau events occurred at $CEM_{43}\approx 2$ min. The lack of additional increase in breathing rate at higher thermal doses suggests a more direct correlation of breathing rate with body temperature, rather than with thermal dose.

Neuronal excitability—Seizures frequently occur in infants who are otherwise healthy but suffering from a fever (febrile seizure). Adults are much more resistant towards developing febrile seizures than infants. Febrile seizure activity is thought to sometimes be generated by hippocampal structures [13], with increased neuronal excitability being related to the likelihood of developing seizures [14]. Liebregts et al. [15] tested the notion that temperature affects synaptic inhibition (mediated by Gamma-aminobutyric acid receptor (GABA-A)) in the juvenile brain in such a way as to increase excitability, and hence presumably the likelihood of developing seizures.

To explore the effects of temperature on neuronal excitability, Liebregts et al. [15] measured neuronal excitability in the hippocampus of adult male Long-Evans rats (6–12 weeks old) and immature rats (15–17 days postnatal) after treating with whole body hyperthermia via heating pad for 10 min. There were two different heating groups: moderate (38.8°C) and severe (40°C). Rats were anaesthetised with an intraperitoneal injection of urethane during treatment. Synaptic drive of inhibitory neurons in several regions of the hippocampus was measured with paired-pulse inhibition. The objective of this study was to identify underlying mechanisms for febrile seizures.

Liebregts et al. focus on two areas: 1) the granule cell layer of the dentate gyrus (DG), and 2) the pyramidal (excitatory) body layer in the hippocampus 'cornu ammonis 1 region', that is usually referred to as CA1. The basic circuit of the hippocampus is with DG providing excitatory synaptic drive onto the excitatory pyramidal cells in region CA3, which provides excitatory synaptic drive to CA1 pyramidal cells (via the Schaffer collaterals). DG itself receives synaptic drive from the entorhinal cortex via the perforant path [16]:

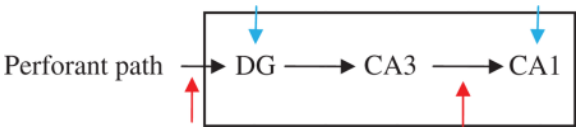

They placed stimulating electrodes (red arrows above) in two places: 1) on the perforant path to drive the cells in DG, and 2) on the cell body layer in CA3, whose axons comprise the Schaffer collaterals, to provide excitatory synaptic drive to pyramidal cells in CA1. They placed extracellular recording electrodes (blue arrows) in two places: 1) in the granule cell layer in DG, and 2) in the pyramidal cell layer of CA1. The amplitude of the activity recorded by such an electrode is thought to be roughly proportional to the number of neurons that synchronously discharge near its vicinity.

For the purpose of this study, it is important to know that inhibitory interneurons exist within each of the hippocampal sub-regions, and these inhibitory neurons connect locally in a 'feedback' fashion. That is, if excitatory pyramidal cells fire action potentials in CA1, for example, they will excite inhibitory interneurons to fire. The interneurons, in turn, synapse back on to the CA1 pyramidal cells that just fired, and inhibit their further firing by release of GABA at their synapses.

Liebregts et al. use paired-pulse inhibition – an electrophysiology method to assess changes in inhibition [15]. The idea is that if a brief electrical stimulus is applied to the Schaffer collaterals, the recording field electrode in CA1 will record a brief negative deflection that represents the firing of the pyramidal cells, called a population spike (pop-spike). To clarify this concept, suppose two brief pulses are delivered in succession. If the timing is just right, the first pulse will cause excitatory pyramidal cells to fire (P1). They, in turn, will cause inhibitory cells to fire that will suppress the firing of their presynaptic pyramidal cells. Since the pyramidal cells are now (briefly) inhibited, the second pulse (which will be set to arrive just at the time that inhibition is maximal) will evoke a lesser response (P2), and the recording electrode will record a smaller pop-spike. One way to quantify the inhibitory effect (as they did here) is to take the ratio of the two pop-spikes, or P2/P1. In this way, the effect of temperature on inhibition can be detected as changes in the ratios of the two pop-spikes.

P1 amplitude (population spike following the first pulse) and P1 onset latency are plotted in Figure 4 (A and B). Predictably, higher CEM_{43} resulted in more change than lower CEM_{43}. The immature rats were treated with a CEM_{43} closer to the lower adult thermal dose (CEM_{43} of 0.035 and 0.042 min, respectively), so age group comparisons should be made at

these lower thermal doses. Hyperthermia treatment results in decreased P1 amplitude in all areas of the hippocampus examined except in the mature rat dentate gyrus (Figure 4A). The most sensitive regions for this endpoint are the immature dentate gyrus and the mature cornu ammonis, which remain ~40% below baseline 30 min after heating. The mature rats seem to be more sensitive to heat stress based on P1 onset latency, specifically the dentate gyrus (Figure 4B).

Their main results, based upon the P2/P1 ratios, indicate that in both young and adult rats inhibition was decreased in CA1 by hyperthermia. Importantly, mild hyperthermia was required to elicit this effect in young rats, but severe hyperthermia was required for adults. Secondly, in adult rats, hyperthermia actually caused an increase in inhibition in the DG, but had no effect in young rats. Since inhibition in CA1 was increased in both young and (to a lesser extent) adults during hyperthermia, increased temperature causes an increase in excitability of this hippocampal region in all ages, by reducing GABA-A synaptic efficacy.

The DG is thought to act like a ‘gateway’ that controls the amount of activity that can pass from high cortical regions into the hippocampus to excite CA3 (which in turn can excite CA1). In adults, inhibition was observed to increase in DG, which they argue can compensate for the decreased inhibition in CA1 by preventing excitatory effects from cortical structures from invading the hippocampus. In contrast, there was no increase (or change) in inhibition in young rats, and so they would not benefit from this DG gating. One could say this study provides evidence that the CA1 region in young brains is more sensitive to hyperthermia than older brains, but that the DG in older brains is more sensitive to hyperthermia than younger brains.

This study raises more general issues regarding the effects of hyperthermia. If the juvenile hippocampus is sensitive to becoming more excitable with increased temperature, then mild hyperthermia might increase the risk in general of having a seizure. Therefore, children already suffering from epilepsy may be more sensitive to hyperthermia.

More generally, this study illustrates that in at least one important brain structure, increases in temperature can differentially affect synaptic transmission in different sub-regions of that structure, in an age-dependent manner. Since the hippocampus is thought to play a role in learning and memory, changes in synaptic efficacies within various sub-regions would be of concern [17]. It may be that inhibitory transmission in other brain regions might be affected in an age-dependent manner by hyperthermia, but this has yet to be studied.

Other effects of heat on CNS—Morrison et al. [18] treated humans with whole body hyperthermia via a liquid conditioning garment (circulating 52°C fluid) and in a hot (35°C) environment for 62 min (average). Subjects were not anaesthetised and had an average rectal temperature of 39°C. A near infrared oximeter was used to monitor/record prefrontal cortex oxygenation and blood volume. Prefrontal cortex haemoglobin was not modified significantly at a CEM_{43} of 0.1 min in humans. This observation also held for levels of oxygenated and deoxygenated haemoglobin.

Racinais et al. [19] obtained a CEM_{43} of 0.15 min in humans via whole body hyperthermia. In that study, humans were subjected to a hot room (50°C and 50% humidity; average wet bulb globe temperature recording 43.1°C) where they walked on treadmills for 10–15 min at 3–5 km/h and then rested in a seated position for 45 min before testing. The average core body temperature was 38.7°C for approximately 120 min. Subjects were not anaesthetised during treatment. This investigation found that heat stress caused significant decreases in muscle torque, drive and spinal modulation in humans. This dose of hyperthermia also caused decreases in the amplitude and latency of electrically evoked action potential, both at

rest and during maximal contraction in the same study. However, it should be noted that this study does not separate the psychological effects of additional stress posed by hyperthermia from the direct effects of hyperthermia on muscles and CNS.

Metabolic effects in the brain

Glutamate, glycine, and GABA—Sharma [5] treated male albino Wistar rats (9–10 weeks old) with whole body hyperthermia using a biological oxygen demand incubator (38°C for 30 min, 1, 2, 3 and 4 h, average core temperature 41°C) without anaesthesia. Glutamate, glycine, and GABA measurements (via HPLC) were made in various regions of the brain to assess the effects of hyperthermia on their concentrations (Figure 5A, B and C, respectively). For all three indicators there tends to be an initial increase in metabolism at a low CEM_{43} (0.115 min) and decrease at a CEM_{43} of 1.29 min. Glutamate is the major excitatory neurotransmitter in the brain. GABA is the major inhibitory neurotransmitter in the CNS, and glycine is the inhibitory transmitter in the spinal cord. Taking the data at face value, all of these major neurotransmitters are perturbed from baseline by hyperthermia, particularly GABA, undergoing a 500%–1000% reduction from baseline at the higher CEM_{43}. Based on these findings, it is difficult to speculate how this translates into changes in the amount of available neurotransmitter at the synapse. Additional investigation is warranted.

Metabolism – Lactate dehydrogenase (LDH) and succinate dehydrogenase (SDH) activity, RNA content, lactate, pyruvate, glutamate, and glycerol levels —Ekimova [20] treated adult male Wistar rats with whole body hyperthermia via a climate chamber (35°C) for 3 h (body temperature 39.3°C). These rats were not anaesthetised during heat treatment. Ekimova et al. made measurements from three nuclei (clusters of cells) in the hypothalamus: (1) the supraoptic nucleus of the hypothalamus that produces the important neuropeptide hormones vasopressin and oxytocin; (2) the paraventricular nucleus of the hypothalamus that plays some role in regulating autonomic functions and appetite; (3) the median preoptic nucleus, involved in thermoregulation. The function of the hypothalamus is to regulate and maintain body homeostasis (body temperature, blood volume, blood pressure, etc.) [21]. Metabolic activity in these hypothalamus regions was assessed by SDH activity, lactate dehydrogenase activity and RNA content. The enzyme activity was assessed in terms of optical density of the end product formazan in neurons, and RNA content was measured using absorption of visible light by stained substrate-stain complexes. As depicted in Figure 6A, enzyme activity and RNA content increased with heating to CEM_{43}=1.07 min. LDH activity increased to a much higher level than the other endpoints of metabolic activity.

Chou et al. [8] treated adult male Sprague-Dawley rats anaesthetised with intraperitoneal urethane with whole body heating via a water blanket for 20–70 min set at 42°C (body temperature range 37.5–41.5°C). Glutamate, glycerol, lactate, and pyruvate levels were measured with a microdialysis analyser. All increased with increasing CEM_{43} indicating increased metabolic activity, but lactate increased at a much higher level even at the lower CEM_{43} examined (Figure 6B). It is noteworthy that extracellular lactate increases dramatically, doubling its value from baseline. Extracellular lactate and pH have been shown to be closely correlated in the brain during other types of treatments [22]. This might suggest deep acidosis in the extracellular space of the hypothalamus as a consequence of hyperthermia, which would be expected to dramatically affect neuronal excitability and function, possibly resulting in cell death [23, 24].

Sympathetic nervous system. Nerve discharge—Kenney et al. [25] monitored renal and splanchnic sympathetic nerve discharge during whole body hyperthermia treatment. Overactivity of renal sympathetic nerve is considered a major cause of the pathophysiology

of hypertension [26, 27]. The splanchnic nerve is thought to influence the regulation of a number of basic functions, such as arterial blood pressure, heart rate, vascular tone [28]. Nerve discharge for three age groups of F344 rats were compared (young (3.3 months), mature (12.6 months), and senescent (24 months)). Rats were treated with whole body hyperthermia via a heat lamp (rectal target temperature 41°C), and neural activity was recorded with a platinum bipolar electrode at the site of the nerve during heating. Rats were not anaesthetised during heat treatment. Nerve discharge increased during the heat exposure in the young and mature rats, whereas no change was observed in senescent rats (Supplementary Figure 3A and 3B). This pattern was observed for both nerve types. Young and mature rats seemed to respond similarly to the heat stress according to the renal nerve discharge data, while the young rats were slightly more sensitive to the increased heat exposure for splanchnic nerve discharge. The study by Kenney et al. showed a surprisingly large increase in firing frequency of these nerves from baseline [25].

Xu et al. [29] assessed thermal damage to the sciatic nerve in adult male Wistar rats (350–400 g). In the rat, the sciatic nerve carries sensory information from the leg (skin, muscles, etc) and was used in this study as a representative model of a typical peripheral nerve that allows for the testing of the effects of heat on both myelinated (A-fibres) and unmyelinated fibres (C-fibres). Rats were anaesthetised with intraperitoneal Hypnorm and midazolam while a heating cuff made of copper tubing with circulating hot water was used to heat the sciatic nerve. The nerve was heated for 20 min at 47°C (heated twice for 10 min with a 30-min interval between heating). The sciatic nerve was stimulated by platinum electrodes. A-fibre and C-fibre action potentials were measured as well as nerve blood flow and plasma adrenaline and noradrenaline. During heat treatment plasma adrenaline and noradrenaline increased significantly 9.9 and 1.5 fold, respectively. Nerve blood flow decreased 56%, and action potentials for A-fibre and C-fibre decreased as well (100% and 45%, respectively). C-fibres are not protected by a myelin layer, hence it is not surprising they were more vulnerable than A-fibres to hyperthermia [30]. These results might suggest that peripheral nerve function in general may be negatively affected by hyperthermia. Xu et al. also observed delayed damage specific to the myelinated nerves resulting from low-grade heating [29]. This would be attributed to the decrease in blood flow since unmyelinated nerves are less vulnerable to ischaemia.

Monafo et al. [31] treated hind limb nerves (sciatic, peroneal, tibial, and sural nerves) of female Sprague-Dawley rats (250–350 g) with local RF (1 MHz, electrodes placed on hind limb) for 60 s until 47°C was reached, and maintained this temperature for an additional 30 s. During RF treatment, rats were anaesthetised with intraperitoneal pentobarbital. Percutaneous measurements of posterior nerve conduction block, conduction velocity, and terminal latency were conducted by inserting electrodes in several regions along the hind limb and recording the waveforms after stimulation. They measured effects of RF heating on: (1) conduction velocity, or the speed that neurons travel down the nerve; (2) conduction block, or the suppression of the ability of the nerve to carry action potentials, and (3) terminal latency, or the time it takes a stimulus at some distal point on the nerve to reach its endpoint, such as its synapse in a muscle. These are all various ways to assess the function of a nerve, and all were affected in the expected directions by heating. Assessment immediately after heat treatment showed an increase in the incidence of complete conduction blocks as well as an increase in terminal latency, and conduction velocity decreased after treatment (Supplementary Figure 3C). Incidence of complete conduction block was increased further 24 h after treatment to 67%, and this level was maintained at the 96 h time point.

Thresholds of thermal damage

Lesion induction and BBB disruption—Several studies have reported threshold data for tissue damage (Figure 7). These papers assess brain lesions and BBB disruption in multiple species (rabbits [32–34], primates [35], and pigs [36]). Heat was administered via either laser or ultrasound. BBB disruption was assessed in ultrasound-treated New Zealand white rabbits by contrast-enhanced MRI in McDannold et al. [32] and with trypan blue penetration in Hynynen et al. [33]. BBB disruption occurred in both studies. Disruption was observed at a lower CEM_{43} value (0.067 min) in the Hynynen et al. study than in the McDannold et al. [32] study (greater than 12.3 min), but at some of the higher CEM_{43} exposures in the McDannold et al. [32] study, disruption was not always observed. The differences in sensitivity may be due to the methods involved in detection. Brain tissue sensitivities may be different between species. A much higher CEM_{43} seems to be required for lesion production in the porcine model [36] (Figure 7B) compared to both rhesus monkeys [35] and rabbits [34] (Figure 7A). Lesions were present after exposure to a similar range of CEM_{43} in rabbits and monkeys even though different heating devices were used.

Summary: Effects of heat on the nervous system—As shown above, damage to the nervous system can be assessed in many different ways. Since the previous report, we have added data at higher CEM_{43}, but the majority of the data fit within the CEM_{43} range of 0 to 20 min. The data show that certain endpoints such as metabolism seem to be more sensitive to heat stress than others, and certain regions of the brain tend to be more sensitive to heat. The majority of the studies did not assess long-term damage, so the permanence/reversibility of the apparent damage or functional changes is unknown. The only exception is the McDannold et al. (2003) threshold study [32] in which brain lesions were detected 5 and 6 weeks after ultrasound treatment. It should be noted that the CEM_{43} in this study was much higher than the majority of the other studies. It is clear that much more work needs to be done to further evaluate the potential for acute and long term damage to the brain, following either total body or focal brain heating.

Effects of heat on testicular physiology and function

Overview

Since the last review in 2001, a number of studies have increased the available knowledge on the effects of hyperthermia on testicular physiology and function. The temperature ranges used in the studies were between 38°C and 43°C, for treatment durations of 15 min to 1 h. Some studies employed fractionated treatments of 30 min each for up to six fractions. All of the heating was performed locally through immersion of the testes in a heated water bath, with the exception of one paper which employed a whole body heating method.

These new data use mouse, rat, and human subjects for evaluation. One general observation is that there appear to be large differences in sensitivity of the testis across species, with human subjects displaying the least sensitivity. Additionally, these new studies highlight the importance of time when assessing thermal damage, as most decreases in testicular functionality are acute and recover over time.

The endpoints used to assess thermal damage in these studies can be classified into six categories: (1) change in testicular mass, (2) fold increase in cell damage, (3) fold increase in cell death, (4) change in testosterone levels, (5) change in sperm characteristics, and (6) alterations in fertility.

Testicular mass

Figure 8A shows the change in testes weight following various heating schemes for two rodent species. The weight of the testes was measured at differing times post-heating to assess permanent or acute changes and define a recovery period [37–41]. Figure 8B clearly shows that human and rat testes are less sensitive to thermal stress than mice.

Mice tend to show a thermal dose-dependent decrease in testicular weight, with as much as a 30–60% loss in mass with CEM_{43}=7.5–15 min [39, 41]. For a low thermal dose of CEM_{43}=0.3 min, the weight quickly recovers within two weeks [39]. At higher doses the weight continues to decrease up to two weeks, but the time frame for recovery is unknown since data were not collected beyond two weeks. In light of the other data showing decreased sperm production and increased cell damage following heat treatments, the testicular mass likely decreases due to cell death and/or decrease in proliferation. The thermal dose delivered in rat studies was much higher than that for mice, at CEM_{43}=180 min [37, 38]. Rats appear to be less sensitive to thermal dose than mice, as this high dose did not cause appreciably more damage than an equivalent mouse dose of CEM_{43}=7.5–15 min. Rats show a consistent deterioration of testicular mass from 1 day post-thermal treatment up to 35 days post-treatment, at which time the damage is persistent to 140 days when analysis concluded. Thus, in this particular case, the damage may be considered permanent.

An important contribution to the testicular data is the study by Wang et al., which assesses a host of functionality and morphology tests in men following scrotal heating (30 min/day for 6 days for a total of CEM_{43}=180 min) [40]. While they did not directly measure testicular weight, they provide relative changes in tubule diameter, tubule volume, and lumen volume 2 and 9 weeks post-treatment. Table III summarises these changes. While these endpoints tend to decrease at 2 weeks, there is complete rebound at 9 weeks. Further, the data at 2 weeks is not statistically significant compared with baseline.

Cell damage

Banks et al. [42] studied the effect of CEM_{43}=7.5 min on DNA damage to motile spermatozoa recovered from the epididymides at a number of time points following treatment, both acute (within 24 h) and later (up to 32 days). DNA damage was assessed using the COMET assay. The amount of DNA damage significantly increased 1 h after treatment and continued to increase until 4 h post-treatment. Within 7 days the DNA damage levels fell to those of the unheated spermatozoa (Figure 9). However, from 7 days to 21 days DNA damage increased and maintained increased levels up to 32 days when the study ended. Due to the transit time of sperm maturation, the DNA damage levels in these spermatozoa are most likely reflective of acute damage to germ cells which is then propagated to mature sperm.

While the above notes the overall increase in levels of DNA damage, not all spermatozoa exhibited DNA damage and therefore Banks et al. also assessed the percentage of motile spermatozoa with any amount of DNA damage. Motile sperm were isolated from the epididymides and assessed for DNA damage. An initial increase in the number of sperm with damage occurred from 4–6 h, fell toward baseline from 1–7 days, and was followed by another increase from 14–32 days. However, the percentage of motile sperm with abnormal DNA at the later periods was higher than the initial 4–6 h increase. From these results it appears that while initially the amount of DNA damage in the most mature sperm is greater, it may be concentrated in fewer spermatozoa, while after two weeks more sperm are likely to have some amount of DNA damage even though the extent of damage present in each spermatozoa is less. These chronic elevated levels of spermatozoa DNA damage suggest

some amount of residual damage to the germ cells. However, this study did not specifically evaluate germ cell damage.

In another study, Paul et al. [39] assessed similar endpoints, but extended the work of Banks et al. to include assessing damage to the germ cell. This study used SCSA to detect the percentage of epididymal sperm with DNA damage over the same time periods but utilising three different thermal doses (Figure 9). The results from Paul et al. are similar to those of Banks et al. in that there is a two-cycle increase in the percentage of epididymal cells with DNA damage, and that this damage increases with increasing thermal dose. However, Paul et al. report a slightly different response time when compared with Banks et al. Paul et al. also investigated the number of DNA lesions in pachytene spermatocytes in the germ cells. This data shows a thermal dose-dependent increase in the number of DNA lesions, evident as early as 3 h post-treatment, peaking in severity around 6–24 h of treatment and maintaining elevated levels of DNA damage up to 14 days. At the 28-day time point, however, DNA damage levels had returned to baseline.

From these two studies it appears that the extent of DNA damage to the spermatozoa and germ cell spermatocytes in mice increases based on thermal dose. This type of damage also appears to consist of two cycles, an initial increase from 4–24 h followed by another increase between 7–14 days. It is unclear whether residual damage exists after 28 days, as the Banks et al. paper suggests lingering residual damage, while the Paul et al. data suggests recovery. This type of damage is likely reflective of underlying germ cell damage. Clearly, further study of this question is warranted. At the current time, no firm conclusion can be drawn regarding whether thermal damage to the testis can lead to permanent DNA damage to spermatozoa. Given the potential genetic risks, this subject requires substantial additional investigation.

Cell death

The effect of heating on testicular cell death has been studied in mice, rats, monkeys, and humans. This data is evaluated over the entire testis with histology (overall cell death in testes) or from an isolated area of the testes, either in the seminiferous tubules or in the testes germ cells. Supplementary Figure 4 shows the increase in cell death over time, following various heating regimens in different species. In mice, Paul et al. [43] showed that whole testis sections stained for caspase 3 positive cells to mark apoptosis had thermal dose-dependent increases in the number of apoptotic cells per histological slice. The amount of cell death peaked at 24 h, decreased slightly at 48 h, but returned to control levels by 7 days post-treatment.

Cell death specifically occurring in the testes germ cells was evaluated both by Banks et al. [42] and Paul et al. [39]. Paul et al. evaluated the number of TUNEL-positive germ cells following three different thermal dose regimens, finding again that the number of apoptotic cells increased with increasing thermal dose. While a thermal dose of CEM_{43}=0.03 min appeared to have elevated cell death at 24 h, this was not statistically significant. At CEM_{43}=0.5 and 7.5 min however, there were significant increases in cell death at 24 h post-heating. Elevated apoptosis levels appeared to persist for longer durations as the thermal dose was increased, with CEM_{43}=7.5 min exhibiting heightened cell death lasting 7 days; but these results were not statistically significant due to a low number of mice studied.

Banks et al. showed different results for the length of increased apoptosis in germ cells. They used a thermal dose of CEM_{43}=7.5 min and similar to the Paul et al. paper, they reported heightened levels of germ cell apoptosis at 24 h. Unlike the Paul et al. paper, they showed elevated apoptotic levels occurring as early as 2 h post-heating and persisting as long as 24 days post-heating. These studies used different mouse models, as mentioned

earlier, and also used different methods for measuring germ cell apoptosis; Paul et al. used TUNEL staining while Banks et al. utilised Apotag staining methods. These studies both indicate an early increase in apoptosis to germ cells within 24 h, but they provide conflicting results on the length of elevated apoptosis. In both situations, however, apoptotic levels return to normal within 28 days and as such this can be taken as a conservative estimate for acute response in mice. These studies underscore that future research may need to evaluate more than one apoptosis assay and add additional time points beyond 28 days to help clarify results.

Perez-Crespo et al. [44] also studied the extent of cell death following testicular heat exposure of CEM_{43}=7.5 min in mice, although they focused on evaluating cell death of mature sperm isolated from the epididymis, determined by TUNEL staining. They found statistically significant increases immediately following heat treatment that persisted up to 28 days and returned to baseline levels by 60 days. The greatest increases in apoptotic epididymal sperm occurred from 14 to 28 days. While this is later than the previous studies, the transit time for maturation from a germ cell spermatocyte to a mature spermatozoa is within 14–28 days. Therefore, detected apoptosis of mature epididymal sperm by Perez Crespo et al. correlates well with the increases at 24 h of apoptosis among testicular germ cells reported by Paul et al. and Banks et al.

In rats, Khan et al. [10] evaluated cell death with TUNEL staining in the seminiferous tubules following CEM_{43}=5.94 min whole body heating. This method of heating is distinct from the other papers investigated, as these assessments were made following whole body heating instead of localised heating. The incidence of apoptotic cells was increased at all time points evaluated, from 2.5 h to the last assessed time point of 24 h post-treatment, peaking at 15 h. This early increase in apoptosis is similar to that seen in mice, with a similar thermal dose sensitivity.

Similar to the elevated thermal doses used to elicit changes in testicular weight, monkeys and humans also require increased thermal doses for a similar cell death effect. Lue et al. [45] used a thermal dose of CEM_{43}=60 min in monkeys, and then evaluated germ cell death with TUNEL staining. Cell death was highest at the first time point assessed, 3 days, gradually decreasing to slightly elevated at 28 days and returning to normal values at the next evaluated time point of 84 days. Apoptotic values remained normal up to the study conclusion at 144 days. This study corroborates earlier emphasis on lower sensitivity to thermal damage and an initial acute apoptotic episode followed by recovery; in monkeys, this recovery occurs by 84 days post-exposure.

Wang et al. [40] studied human subjects with a thermal dose of CEM_{43}=180 min, and also investigated germ cell death in the testes with TUNEL staining, at two weeks post-heating. While this study evaluated only one time point, this damage assessment agreed with the study in monkeys, as shown in Supplementary Figure 4.

In summary, cell death following thermal exposure to the testes appears to be transient, occurring mostly in the first 24 h following exposure. In mice and rats, levels of apoptosis appear to return to baseline levels as early as one week, but can take as long as 28 days. In mice, there may be a threshold dose for testicular germ cell death, as mice exposed to only CEM_{43}=0.03 min trended towards but did not show a statistically significant increase in apoptotic cells. However, further evidence for a possible threshold thermal dose is warranted. Monkeys and humans appear to be less sensitive to cell death than mice, but one cannot discount the possibility that the testicular temperature in humans was lower than mice, as previously discussed. Monkeys exhibit full recovery between 28 and 84 days. It is difficult to know the temporal response of human testes for these endpoints as only one time

point was assessed. However, this time point correlates with the monkey damage–time curve.

Testosterone levels

Testosterone levels and related indicators have been analysed in mice, rats, monkeys, and humans, with endpoints of both serum testosterone levels and percentage of testosterone positive Leydig cells. Data for mice are scarce, with only one data point assessed 24 h after CEM_{43}=15 min [41]. This shows substantial decrease in testosterone levels, even at this early time point. In rats, the percentage of testosterone positive Leydig cells decreases dramatically at day 1, similar to the mouse study, but follow up data show a subsequent recovery period lasting until 140 days, at which time the study ended but full recovery was not achieved [37, 38] (Supplementary Figure 5).

In monkeys, serum testosterone was significantly decreased at two weeks post-exposure, with subsequent continual recovery to baseline levels between 12 and 20 weeks [45, 46]. Results in monkeys seem counterintuitive, as the higher CEM_{43} produced less apparent damage than the lower CEM_{43} (Supplementary Figure 5). However, these studies only had a few monkeys per study (3–4) and showed large variances and fluctuations in serum testosterone levels between and within monkeys. What is important to note is the initial amount of damage is similar at both thermal doses, with a large decrease detected at the earliest assessed time point of 2 weeks that does eventually recover without residual damage between 12 and 20 weeks. Again showing increased resistance to testicular heat damage, human subjects had no significant decrease in serum testosterone levels at any assessed time point, from 3 to 30 weeks [40].

Sperm characteristics

A myriad of sperm characteristics were assessed following heating, including number of sperm in ejaculate, sperm viability, sperm motility, and the percentage of sperm with normal morphology. These were assessed in two studies, one by Perez-Crespo et al. [44] that evaluated sperm characteristics in mice after CEM_{43}=7.5 min, and the other by Wang et al. [40] which evaluated humans exposed to CEM_{43}=180 min.

In mice, the sperm concentration in ejaculate decreased immediately after heating, continuing to decrease in concentration until 28 days later, with persistent damage until the last follow-up time point of 60 days, as shown in Figure 10. Sperm viability and motility showed similar decreases, starting either immediately or by 7 days, and increasing in severity until 21–28 days after heat treatment. Both motility and viability then recovered, with almost complete recovery at the 60 days termination of study.

In humans the first assessment occurred at 3 weeks from heat treatment initiation. Damage trends were similar in all three sperm characteristics assessed: sperm concentration in the ejaculate, sperm motility, and percentage of sperm with normal morphology. At three weeks all three end points showed decreases from baseline, with a dramatic 62% reduction in sperm ejaculate concentration, while the two other endpoints had minimal reductions. Damage continued to progress in all areas up to 9 weeks, when all of the markers of damage started to recover. Sperm ejaculate concentration and sperm motility fully recovered by 12 weeks and 18 weeks, respectively. The percentage sperm with normal morphology almost recovers fully by 22 weeks, but may have some residual damage that persists; from the provided data this is unclear and an area in need of further investigation.

Fertility

The fertility of male mice after testicular heating was also investigated, using a low thermal dose of CEM_{43}=0.5 min [39] or a mid-range dose of CEM_{43}=7.5 min [44]. Male mice underwent testicular heating and then were allowed to copulate with female mice at various times following their heat treatment. The success of breeding was then compared to unheated mice, assessed by the number of pregnant females per male mouse, the average number of foetuses produced by females impregnated from heated mice, and the number of implantation sites per female impregnated from heated mice. These results are presented in Supplementary Figure 6. From Paul et al. [39], the lower CEM_{43}=0.5 min did not affect the number of females that a heated male could impregnate, but did decrease slightly the number of foetuses per pregnant female, from 7–8 in the controls to 6–7 in the lower thermal dose group. In the higher thermal dose group the results were more dramatic, with foetus numbers dropping to around 1 per impregnated female. Along these lines, the higher dose also saw deterioration in the number of females a heated male could impregnate. These results were assessed for males allowed to copulate between 22–28 days after heating.

In a study by Perez-Crespo et al. [44], male mice were subjected to CEM_{43}=7.5 min and then the effect of time to copulation on male fertility was assessed. In this study, decreases in average number of foetuses per impregnated female and number of implantation sites per female were directly related with time. Decreases of 29% and 35% of implantation site number and foetus number was observed, respectively, for male mice that copulated with female mice between 0 and 7 days post-heating. These numbers slightly increased when mice copulated at day 14 post-heating, and decreased to lowest levels of 46% and 51% when mice copulated 21–28 days after heating.

The study by Perez-Crespo et al. showed a dramatic deterioration in fertility of male mice 21–28 days after heating, similar to the study by Paul et al., although the results demonstrated slightly less fertility decrease for the same thermal dose. These results correspond to the maximum decreases seen in characteristics of sperm functionality, such as motility, viability, and concentration (Figure 10). Unfortunately, this study did not assess time points after 28 days, so there is not enough information to predict whether decreases in fertility are transient or prolonged. Further, as mice are much more sensitive in the other areas of testicular damage, it is difficult to predict what the effect on humans would be.

Summary: Effects of heat on testicular physiology and function

In summary, many important additions in the effects of heating on testicular damage have been made since the previous review paper. From these new data it is apparent that monkeys and humans may be more resistant than mice to thermal damage, and that damage inflicted by heating is for the most part acute with recovery occurring within a week to many weeks. It appears that most of the recovery is without residual damage, although in some cases this is unclear.

An important area for future research is to focus on better thermometry of the testis. From the results shown one could conclude that the human testis is more thermally resistant than the rat. However, one has to consider that the actual temperature of the human testis is probably lower than that of the rat and mouse, given the method used for heating, which was the same in both cases (water bath immersion). The physical difference in the size of the organs and the perfusion likely affected the actual organ temperature, since any temperature elevation would be entirely dependent upon thermal conduction. The temperature of the testis was not measured in either case, so a direct comparison cannot be made. A further complication is that the human study involved multiple heat treatments. Adaptive responses to prior heating, possibly involving the heat shock response, may have blunted any effect

that might have been seen after a single treatment. Further analysis with direct tissue measurements or heat transfer models to assess actual thermal dose accumulation in the testis is warranted.

Effects of heat on other tissues

Overview

In addition to testes and brain, we found various studies containing thermal damage data in 17 different tissue types. These were categorised into percentage damage (liver, skin, bone, muscle, and bladder), percentage damage with whole body heat treatment (kidney, bone marrow, thymus, liver, muscle, and intestine), damage threshold (oesophagus, liver, muscle, prostate, kidney, cornea, retina, eyelids, ear, and skin), and damage threshold with whole body heat treatment (muscle, small intestine, and mammary gland). Some papers contained either both percentage damage and threshold data or thermal damage data from various tissues types. We discussed thresholds for thermal damage previously in most tissue types. For those tissues we compared new data with what we reported previously. In addition, we added new data on bone, thymus, and mammary gland.

Update (2002–present) on tissues included in the previous review

Liver. Local heating—In our previous review we reported that CEM_{43}=41–80 min and CEM_{43} greater than 80 min caused acute and minor damage to liver tissue. Since then, further studies were done to determine thermal tissue damage at CEM_{43}>80 min. The study by Seror et al. [47] showed that CEM_{43}=320 min, delivered using radiofrequency (RF) ablation is enough to cause thermal coagulation of pig liver. Damage was assessed by gross and histopathological observation as well as MR imaging. In the other studies heat treatment by RF ablation [48, 49] and high intensity focused ultrasound (HIFU) [50, 51] at higher CEM_{43} between 2×10^5 and 8.6×10^{11} min also caused tissue necrosis in rabbit [49] and pig [48, 50, 51]. However, CEM_{43} for actual threshold of damage could not be determined due to the lack of temperature information at the edge of the thermal lesion. Therefore, both in our previous and current review we were not able to obtain the true threshold of thermal damage due to the lack of information at CEM_{43} between 80 and 320 min.

Whole body hyperthermia—In one study, whole body hyperthermia was performed by venoarterial perfusion in dogs [52]. Using the perfusate warmed to 44–45°C, the dogs' rectal temperature was elevated to ≥42°C for 4 h, resulting in a thermal dose of CEM_{43}=61 min. Immediately and 7 days after treatment possible liver damage was assessed by serum biochemical changes. Though moderate increase of various biochemical parameters was observed, only aspartate transaminase (AST) and alkaline phosphatase remained elevated 7 days after the treatment. This suggests that systemic hyperthermia at CEM_{43}=61 min caused only acute and minor functional damage in the liver.

Bladder—We previously reported that CEM_{43} greater than 80 min resulted in chronic and significant thermal damage in dog bladder. Here we found one additional study investigating the functional damage of bladder by assessing its volume capacity in rats [53]. Microwave applicators were used to achieve temperatures of 41°, 42°, 43°, 44°, and 45°C for 1 h. Observations were made up to 28 days after treatment. At CEM_{43}=11.2 min, there were no immediate changes in bladder volume capacity. On the other hand, CEM_{43}=57 min showed significantly decreased bladder volume capacity on days 1 and 3. Though bladder capacity recovered by day 10, transient reduction was observed again on day 21. Heat treatment at 45°C likely yielded CEM_{43} of around 120 min, and resulted in a further decrease in bladder volume capacity in surviving rats. However, many animals died in this treatment group,

suggesting that CEM_{43}≈120 min is a lethal dose. Due to the lack of pathologic data, it is not clear whether high mortality was due to severe damage in bladder or in other organs.

In conclusion, our previous and current reviews reported that in terms of thermal dose, CEM_{43}=11.2 min was below the threshold of thermal damage to bladder, CEM_{43}=57 min caused functional damage, CEM_{43}>80 min resulted in chronic and significant damage, and CEM_{43}≈120 min was lethal.

Skin. Local heating—In our previous review, heat treatment at CEM_{43} between 21 and 40 min induced acute and minor damage to skin function. At CEM_{43}>41 min, significant acute and chronic damage was apparent. Our previous review also indicated that complete necrosis in human skin occurs at CEM_{43} between 288 and 1.5×10^4 min [1].

In a new study using a light emitting diode there were no burns on human skin at CEM_{43}=240 min [54]. However, heat at CEM_{43} between 480 and 960 min caused immediate superficial burns. In terms of CEM_{43} resulting in complete skin necrosis, this study was consistent with our previous review (Supplementary Figure 7).

A study by Werner et al. [55] examined thermal damage to human skin in more detailed ways. Skin was heated using contact thermodes at a dose of CEM_{43}=112 min (7 min heating at 47°C). In this study, authors observed not only acute and significant increase in skin erythema, but also changes in functional responses. After heat treatment, thresholds for warm and cold detection were increased while heat and mechanical pain thresholds were decreased. In terms of pain responses, both heat pain and mechanical pain responses were increased after heating. In particular, responses to mechanical pain immediately increased both inside and outside the burn areas. However, they returned to basal levels within 4 h, while heat pain responses stayed elevated.

In contrast to the papers discussed above, Landsberg et al. [56] showed beneficial effects of heat on granulation tissue (GT) formation in the rat. In this study, skin was excised first and GT developed in the wound area. On day 5 hyperthermia was given using a diode laser, and 3 days after heat treatment the thermal effect was examined. CEM_{43} ranged from 2 to 256 min. In general, heat treatment decreased GT formation. In particular, treatment at temperatures between 47° and 50°C was sufficient to cause significant effects. However, at temperatures higher than 50°C, thermal coagulation occurred in underlying muscle.

Muscle

Local heating—Muscle damage was assessed by indicators such as blood creatine levels and neuromuscular function, as well as appearance of haemorrhage and necrosis. In our previous review, when CEM_{43} was between 41 and 80 min, there was acute but minor damage to muscle. At CEM_{43} higher than 80 min, damage (haemorrhage and necrosis) became more chronic and significant.

Heat treatment by microwaves to a thermal dose of CEM_{43}=26 min was not enough to induce thermal damage, which was assessed by blood creatine kinase levels and tissue histology in humans [57]. On the other hand, HIFU caused muscle damage in the pig at CEM_{43} at 0.25 and 103 min [58]. Haemorrhage and tissue damage were observed 0–4 h after treatment. On day 2, segmental necrosis was observed followed by recovery within 7 to 14 days. Another study also showed that HIFU at CEM_{43}=283 min caused thermal lesions in pig muscle immediately after treatment [51]. Higher CEM_{43} achieved using ultrasound (between ~650 and 1.9×10^{10} min) [59] or using HIFU (between 1.1×10^3 and 7.6×10^4 min) [60] resulted in tissue necrosis in rabbit.

Lack of thermal damage in the study using CEM_{43} lower than 40 min (CEM_{43}=26 min) [57] was consistent with what we previously reported, but tissue damage observed after HIFU treatment at CEM_{43}=0.25 min was not [58]. However, considering that HIFU intensity was as high as 4390 W/cm^2 when CEM_{43}=0.25 min was achieved, this effect is likely due to cavitation (bubble formation due to deposition of acoustic power) rather than temperature elevation (Supplementary Figure 8). The authors also detected signs of cavitation in the heated areas where tissue damage was observed.

In addition to thermal tissue damage, we also found a study by Nosaka et al. that showed beneficial heat effects on neuromuscular function [61]. Microwave diathermy treatment was given to upper arms of human subjects at CEM_{43}=2.17 min. One day after treatment, eccentric actions of the elbow flexors were performed. While no difference was observed before the exercise, the rates of post-exercise recovery of both maximal isometric strength (MVC) and range of motion (ROM) were significantly greater in the heated group. These effects lasted for 4 days. On the other hand, muscle soreness upon extension significantly decreased between days 2 and 4 after exercise. Muscle soreness upon palpation and flexion did not show any significant difference compared to the control groups. This study also measured plasma creatine kinase (CK) and myoglobin, which can suggest thermal damage to muscle. No changes were seen in either of these parameters. In summary, this study determined that heat treatment at low CEM_{43} such as 2.2 min increased muscular function and decreased muscle soreness without significant tissue damage.

Whole body heating—A study by Morrison et al. examined neuromuscular function after whole body heat treatment with a liquid conditioning garment in humans [62]. Subjects were divided into three groups according to their physical fitness: highly fit, moderately fit, and low fit groups. After giving heat with a liquid conditioning garment at CEM_{43} between 0.17 and 0.18 min, maximal voluntary isometric contraction (MVC) and voluntary neuromuscular activation (VA) were assessed. Both MVC and VA decreased at higher CEM_{43} but there was no significant difference among the three baseline fitness groups.

Kidney—We previously reported that CEM_{43} below 20 min caused acute minor thermal damage in the kidney. In the current review we found tissue damage reported at higher CEM_{43} between 70 and 2.3×10^{19} min. He et al. heat-treated pig kidney at CEM_{43} between 70 and 7.2×10^{4} min using microwaves [63]. On days 2 and 7, tissue damage in the heated region ranged from thermal fixation to coagulative necrosis, and was observed at all doses with histology. At higher CEM_{43} severity of damage increased. RF ablation at much higher CEM_{43} (between 5.4×10^{9} and 2.3×10^{9} min) also caused coagulative necrosis in pig [64, 65] and dog [66] kidney immediately or 3 days after treatment.

In conclusion, based on our previous and current reports, CEM_{43} above 70 min resulted in acute and significant damage (up to and including coagulative necrosis), while acute and minor damage was observed at CEM_{43} below 20 min. However, we were not able to find data in the range between 20 and 70 min.

Prostate—Previously we reported that CEM_{43} higher than 80 min is required to cause both minor and significant acute damage to the prostate [1]. In accordance with that, our newly found studies determined that CEM_{43}=240 min was the thermal damage threshold while CEM_{43}=50 min was below the threshold in dog when treated with interstitial [67, 68] or transurethral [67, 69–72] ultrasound applicators. In these studies tissue damage was assessed by MR imaging and confirmed by histology. They also included thermal data and CEM_{43} measured by MR imaging.

In conclusion, these new data further refine the dose range where significant thermal damage is expected; CEM_{43}=50 min is below threshold, CEM_{43}=80 min causes minor damage, and CEM_{43}=240 min results in complete coagulation (Supplementary Figure 9).

Eye

Local heating: Cornea—In our previous review we reported that heat treatment causes acute and minor damage at CEM_{43} between 21 and 40 min and acute and significant damage at CEM_{43}>41 min. In this review we found a report on thermal damage in rabbit cornea following ultrasound heating [73]. While CEM_{43}=0.026 min caused no damage, CEM_{43}=21.3 min resulted in mild and acute effects in cornea (epithelial cell oedema, collagen disorganisation, severe stromal oedema, intrastromal vacuole formation, plump keratocyte nuclei, and endothelial cell detachment). When CEM_{43} increased to 2.2×10^4 min, severe corneal damage was observed immediately and 7 days after treatment. On the other hand, a functional study showed that CEM_{43}=0.313 min administered using an eyelid-warming sheet gave beneficial effects on cornea by improving near vision immediately after treatment [74]. Study subjects were extensively exposed to diffuse light reflections from computer screens. This study also showed that with eyelid hyperthermia both objective and subjective accommodation increased. Subjective accommodation further increased 90 min after treatment, while objective accommodation began to decrease. This study indicates that periocular hyperthermia at a low CEM_{43}=0.313 min has beneficial effects in work-related eye dysfunction.

Local heating: Retina—Previously we reported on a study in rabbits that showed chronic and minor damage at CEM_{43}<21 min, acute and minor damage at CEM_{43}=21–40 min, and acute and significant damage at CEM_{43}>41 min. In a new study we found CEM_{43} between 0.02 and 1.5 min did not cause any thermal damage to the rabbit retina when administered using a non-invasive transpupillary diode laser [75]. Acute thermal lesions were observed at CEM_{43} as high as 926.2 min. These results are consistent with our prior report, and they establish that CEM_{43} of less than 1.5 min does not cause detectable thermal damage (Figure 11).

Local heating: Eyelids—According to our previous report, heating eyelids at CEM_{43} between 21 and 40 min causes acute and minor damage. In this review a study by Blackie et al. showed that heating eyelids using the warm compresses at CEM_{43} between 0.015 and 34.54 min did not induce any thermal damage in humans [76].

In summary, CEM_{43}=21.3 min caused mild thermal damage and severe coagulation occurred at 2.2×10^4 CEM_{43} in rabbit cornea [73] (Figure 11). This is somewhat consistent with what we reported previously, with mild and acute damage occurring at CEM_{43}=21–40 min and acute and significant damage occurring at CEM_{43}>41 min. The threshold for damage to the rabbit retina is between CEM_{43}=2 and 926 min. There were no data to indicate a threshold for damage to eyelids, beyond that which we reported previously in humans.

Oesophagus

Local heating—While our previous study showed that CEM_{43} lower than 20 min resulted in acute and significant damage to the oesophagus, a newly found study showed that giving heat at CEM_{43}=278 min using an ultrasound applicator caused necrosis in pig oesophagus [77]. We did not find any thermal damage information at CEM_{43} between 20 and 278 min.

Bone marrow

Whole body heating—Whole body hyperthermia at CEM_{43}=15 min using a dry-air incubator showed significant increase of cell death in rat bone marrow [11]. This study correlates with our previous review that also showed both minor and significant acute damage at CEM_{43} lower than 20 min.

Small intestine

Whole body heating—In our previous review, CEM_{43} lower than 20 min induced acute (evaluated at less than 30 days) and significant damage in the small intestine. At CEM_{43} above 80 min, significant and chronic (evaluated later than 30 days post-treatment) damage was observed.

A newly found study examining correlation of whole body heat treatment and the intestinal permeability in rats showed results consistent with our previous report [78]. Small intestinal permeability was assessed by plasma FITC dextran (FD-4) levels (Supplementary Figure 10). At CEM_{43}=1.5 and 4.6 min, permeability began to increase and showed significant changes at CEM_{43}=8.9 min. At this thermal dose, severe tissue damage was also observed, which was consistent with our previous report.

We additionally found a study that determined heat effect on ischaemia/reperfusion-induced tissue damage in the rat [79]. In this study whole body hyperthermia was given at CEM_{43}=7 min. Ischaemia (60 min) was induced by occluding the mesenteric artery followed by 120 min of reperfusion. Immunohistological data showed that heat treatment caused a 2-fold decrease in intestinal tissue damage induced by ischaemia/reperfusion. Although ischaemia decreased β-ATP levels in both control and heat treatment group, the heated group showed fast and better recovery of β-ATP levels by reperfusion. Along with increased Hsp72 levels detected in the heated group, this indicates that hyperthermia protects tissues from ischaemia/reperfusion injury, possibly through induction of heat shock protein.

Tissues not included in the previous review

Bone

Local heating: Rabbit bone was treated by heating a titanium implant previously inserted into the tibia [80]. Thermal doses were CEM_{43}=16, 80, and 128 min. Thirty days after treatment, bone damage was assessed grossly. At CEM_{43}=16 min irreversible bone resorption was observed and as CEM_{43} increased, the percentage of irreversible bone resorption was also increased (Supplementary Figure 11).

Thymus

Whole body heating: Whole body hyperthermia at CEM_{43}=15 min using a dry-air incubator increased cell death in rat thymus [11]. In this study apoptotic rates in thymus cells were assessed using TUNEL staining 10 h after treatment. Another whole body hyperthermia study showed that CEM_{43}=6 min was sufficient to induce cell death in both rat thymus medulla and cortex [10]. Cell death which was also examined by TUNEL staining at different time points was the highest at 10 h after treatment. Within 24 h, apoptosis rates returned to baseline.

Mammary gland: Heat treatment using a balloon catheter caused thermal damage to goat mammary gland [81]. When the catheter inside the balloon was heated to 87–90°C, temperatures outside the balloon in the breast tissue were 45–55°C. In this study, the correlation between the treatment time and the size of necrosis was determined. However,

due to the lack of time and thermal information, we could obtain only one CEM_{43} value (28.3 min) which was high enough to cause thermal damage.

Ear: We found two papers examining the effects of whole body hyperthermia on inner ear function in mouse [82, 83]. The main purpose of these papers was to investigate the heat-induced ear protection from acoustic injury. Yoshida et al. [82] showed that CEM_{43}=1.9 min before sound exposure protected ear from permanent threshold shift (PTS). This effect was significant when the heat-sound interval was 6–12 h. To determine whether it is due to thermal alteration of ear function, cochlear function was investigated by measuring compound action potential (CAP) from right cochlear and distortion product otoacoustic emission (DPOAE), which represents functional effect on the middle ear and the contribution of outer hair cells (OHCs). This study concluded that there were no detectable changes in ear function after heat treatment.

A later study by Murakoshi et al. [83] tried to determine whether heat changes OHCs. When whole body hyperthermia was given at CEM_{43}=1.9 min, Young's modulus and F-actin of OHCs were increased. Their increase peaked either 3–6 h or 12 h after treatment and returned to basal levels within 48 h. The results indicated that DPOAE increased when mice were exposed to sound after heat treatment, which also suggests the protective effect of heat against acoustic injury.

Summary: Effects of heat on other tissues—Our current report showed consistency with our previous review in terms of thermal doses that cause tissue damage. A variety of heating methods were used in the studies reviewed here, and thermal doses varied widely for various tissues. For the most part it is important to distinguish total body from local heating and we have pointed out all cases where total body heating was used. Some of the studies further refined thermal damage thresholds (bladder, prostate). However, in some tissues we could not find values of CEM_{43} that delineated thresholds between absence and presence of damage (kidney, liver and retina). In addition to studies of tissue damage, we also found studies that revealed beneficial effects of heat treatment on tissue function.

Summary and future directions

This report summarises the most recent findings on thermal damage in various tissues. Nervous system data of this type are mostly available in the lower range of thermal doses (CEM_{43}<20 min), with damage being assessed shortly after treatment. The brain is altered in a variety of ways at different thermal doses, with metabolism being altered at much lower doses than other indicators. Various regions of the brain experience differing degrees of sensitivity to heat damage, and whole body hyperthermia can modify brain function differently for animals of different ages. Testicular damage may occur in monkeys and humans at much higher thermal doses than in mice, but lack of accurate thermal data in the testis precludes a firm conclusion on this point. Available long-term assessment data (CEM_{43}<20 min) shows that most heat damage at low doses is reversible in the testes. Aside from brain and testes, we also summarised effects of a wide range of thermal doses on tissue damage and function in several other organs.

Accurate thermometry at the lesion site

While a myriad of new data has become available since we last published a review on this subject [1], most of the recent publications we found do not provide enough data for an accurate assessment of thermal tissue damage. This was mostly due to insufficient temperature and/or damage data and lack of co-registration of such data. Lack of adequate thermal history data is a tremendous and frustrating handicap. For example, measurement of surface temperature is not sufficient for knowing the temperature inside an organ. This was a

problem in interpreting the data on testicular damage from heating. In other cases, such as in the case of brain damage assessment, temperature in the ear canal was measured. This is not likely an accurate assessment of brain temperature. Furthermore, exact location of heating must be considered in complex organs, where the same thermal dose may result in vastly different degrees of damage in different regions (data on the brain is a good example). Novel non-invasive thermometry techniques as well as modelling approaches may provide new ways to approximate local temperature. We hope that in the future, more authors will measure temperature in the exact spot where the tissue damage is assessed.

Importance of the isoeffect—Current literature assesses a variety of damage types and functional effects of heat. Wherever comparisons have been made, it is apparent that the effect depends on the thermal dose. Therefore it is important that future research focuses on collecting multiple temperature–time and damage data that yield isoeffects. For example, such data would allow estimates of the time of heating at 45°C or at 50°C that would be needed to achieve tissue necrosis. This type of data collection is necessary for meaningful comparisons of studies, and in the broader context, such data are essential for establishing thermal exposure and treatment guidelines.

Thermal dose—A well-established relationship between thermal dose and tissue damage exists. While a sizeable body of literature describes tissue effects at thermal doses less than CEM_{43}=40 min, there are insufficient data in the range CEM_{43}=40–300 min for many tissues. This should be addressed in future research in order to improve thermal dosimetry during treatment as well as to determine levels of safe exposure.

Assessment time—This report clearly shows that severity of tissue damage depends not only on the thermal dose, but also on the time after exposure at which damage is assessed. There is currently a lack of data of chronic effects of heat exposure, for which thermal dose could be calculated. For example, brain data of this type are especially scarce. Therefore, we recommend that future studies evaluate damage over a range of assessment times.

Importance of in vivo measurements—This report excludes all *ex-vivo* data on thermal damage, despite an abundance of such data. Excised tissue likely reacts differently to thermal exposure, in that it is not perfused with nutrient and oxygen-rich blood that also heterogeneously cools it. In addition to these differences in the *in vivo* and *in vitro* experimental environments, our examination of literature shows that the majority of *in vitro* studies were done without proper care for the condition of tissue prior to heat exposure.

Importance of human data—For all of the tissues we reviewed, very little data that permits thermal dose calculation is available for humans, and most of the data we reviewed here concerns rodents. Here, as well as in the previous review, we indicated that inter-species differences in tissue sensitivity to thermal stress exist. Therefore, it is imperative that, where possible, thermal history at the site of heating should be recorded during clinical trials and treatments. With the recent advancements in noninvasive thermometry, we hope that such data will be more widely accessible in the near term.

Supplementary Material

Refer to Web version on PubMed Central for supplementary material.

Acknowledgments

Declaration of interest: This work was supported by a grant from the NIH//NCI (CA42745-22 and -23), NIH Biotechnology Training Grant T32GM008555, by the DOD and a contract from the Mobile Manufacturers Forum and the GSM Association (GSMA). The authors alone are responsible for the content and writing of the paper.

References

1. Dewhirst MW, Viglianti BL, Lora-Michiels M, Hanson M, Hoopes PJ. Basic principles of thermal dosimetry and thermal thresholds for tissue damage from hyperthermia. Int J Hyperthermia. 2003; 19:267–294. [PubMed: 12745972]
2. Sapareto SA, Dewey WC. Thermal dose determination in cancer therapy. Int J Radiat Oncol Biol Phys. 1984; 10:787–800. [PubMed: 6547421]
3. Wiart M, Curiel L, Gelet A, Lyonnet D, Chapelon JY, Rouviere O. Influence of perfusion on high-intensity focused ultrasound prostate ablation: A first-pass MRI study. Magn Reson Med. 2007; 58:119–127. [PubMed: 17659632]
4. Kiyatkin EA, Sharma HS. Permeability of the blood–brain barrier depends on brain temperature. Neuroscience. 2009; 161:926–939. [PubMed: 19362131]
5. Sharma HS. Hyperthermia influences excitatory and inhibitory amino acid neurotransmitters in the central nervous system. An experimental study in the rat using behavioural, biochemical, pharmacological, and morphological approaches. J Neural Transm. 2006; 113:497–519. [PubMed: 16550328]
6. Noor R, Wang CX, Shuaib A. Hyperthermia masks the neuroprotective effects of tissue plaminogen activator. Stroke. 2005; 36:665–669. [PubMed: 15705940]
7. Cremer OL, Diephuis JC, van Soest H, Vaessen PH, Bruens MG, Hennis PJ, Kalkman CJ. Cerebral oxygen extraction and autoregulation during extracorporeal whole body hyperthermia in humans. Anesthesiology. 2004; 100:1101–1107. [PubMed: 15114206]
8. Chou YT, Lai ST, Lee CC, Lin MT. Hypothermia attenuates circulatory shock and cerebral ischemia in experimental heatstroke. Shock. 2003; 19:388–393. [PubMed: 12688553]
9. Mustafa S, Elgazzar AH, Essam H, Gopinath S, Mathew M. Hyperthermia alters kidney function and renal scintigraphy. Am J Nephrol. 2007; 27:315–321. [PubMed: 17495428]
10. Khan VR, Brown IR. The effect of hyperthermia on the induction of cell death in brain, testis, and thymus of the adult and developing rat. Cell Stress Chaperones. 2002; 7:73–90. [PubMed: 11892990]
11. Belay HT, Brown IR. Spatial analysis of cell death and Hsp70 induction in brain, thymus, and bone marrow of the hyperthermic rat. Cell Stress Chaperones. 2003; 8:395–404. [PubMed: 15115291]
12. Schuchmann S, Schmitz D, Rivera C, Vanhatalo S, Salmen B, Mackie K, Sipila ST, Voipio J, Kaila K. Experimental febrile seizures are precipitated by a hyperthermia-induced respiratory alkalosis. Nat Med. 2006; 12:817–823. [PubMed: 16819552]
13. Dube CM, Brewster AL, Richichi C, Zha Q, Baram TZ. Fever, febrile seizures and epilepsy. Trends Neurosci. 2007; 30:490–496. [PubMed: 17897728]
14. Bernard C, Cossart R, Hirsch JC, Esclapez M, Ben-Ari Y. What is GABAergic inhibition? How is it modified in epilepsy? Epilepsia. 2000; 41(S6):S90–S95. [PubMed: 10999527]
15. Liebregts MT, McLachlan RS, Leung LS. Hyperthermia induces age-dependent changes in rat hippocampal excitability. Ann Neurol. 2002; 52:318–326. [PubMed: 12205644]
16. Brown, TH.; Zador, AM. Hippocampus. In: Shepherd, GM., editor. Synaptic Organization of the Brain. third edition. New York: Oxford University Press; 1990. p. 346-388.
17. Cohen, NJ.; Eichenbaum, H. Memory, Amnesia, and the Hippocampal System. Cambridge, MA: MIT Press; 1993.
18. Morrison SA, Sleivert GG, Neary JP, Cheung SS. Prefrontal cortex oxygenation is preserved and does not contribute to impaired neuromuscular activation during passive hyperthermia. Appl Physiol Nutr Metab. 2009; 34:66–74. [PubMed: 19234587]
19. Racinais S, Gaoua N, Grantham J. Hyperthermia impairs short-term memory and peripheral motor drive transmission. J Physiol. 2008; 586:4751–4762. [PubMed: 18703579]

20. Ekimova IV. Changes in the metabolic activity of neurons in the anterior hypothalamic nuclei in rats during hyperthermia, fever, and hypothermia. Neurosci Behav Physiol. 2003; 33:455–460. [PubMed: 12921176]
21. Swanson LW, Sawchenko PE. Hypothalamic integration: Organization of the paraventricular and supraoptic nuclei. Annu Rev Neurosci. 1983; 6:269–324. [PubMed: 6132586]
22. Scheller D, Kolb J, Tegtmeier F. Lactate and pH change in close correlation in the extracellular space of the rat brain during cortical spreading depression. Neurosci Lett. 1992; 135:83–86. [PubMed: 1542441]
23. Ying W, Han SK, Miller JW, Swanson RA. Acidosis potentiates oxidative neuronal death by multiple mechanisms. J Neurochem. 1999; 73:1549–1556. [PubMed: 10501200]
24. Staub F, Mackert B, Kempski O, Peters J, Baethmann A. Swelling and death of neuronal cells by lactic acid. J Neurol Sci. 1993; 119:79–84. [PubMed: 8246014]
25. Kenney MJ, Fels RJ. Forebrain and brain stem neural circuits contribute to altered sympathetic responses to heating in senescent rats. J Appl Physiol. 2003; 95:1986–1993. [PubMed: 12882996]
26. DiBona GF, Kopp UC. Neural control of renal function. Physiol Rev. 1997; 77:75–197. [PubMed: 9016301]
27. Malpas SC, Ramchandra R, Guild SJ, McBryde F, Barrett CJ. Renal sympathetic nerve activity in the development of hypertension. Curr Hypertens Rep. 2006; 8:242–248. [PubMed: 17147923]
28. Sato MA, Morrison SF, Lopes OU, Colombari E. Differentiated hemodynamic changes controlled by splanchnic nerve. Auton Neurosci. 2006; 126-127:202–210. [PubMed: 16567132]
29. Xu D, Pollock M. Experimental nerve thermal injury. Brain. 1994; 117:375–384. [PubMed: 8186963]
30. Patton, HD.; Fuchs, AF.; Hille, B.; Scher, AM.; Steiner, R. Textbook of Physiology: Exciable Cells and Neurophysiolgy. 21st edition. Philadelphia: Saunders; 1989.
31. Monafo WW, Eliasson SG. Sciatic nerve function following hindlimb thermal injury. J Surg Res. 1987; 43:344–350. [PubMed: 3657138]
32. McDannold N, Vykhodtseva N, Jolesz FA, Hynynen K. MRI investigation of the threshold for thermally induced blood–brain barrier disruption and brain tissue damage in the rabbit brain. Magn Reson Med. 2004; 51:913–923. [PubMed: 15122673]
33. Hynynen K, McDannold N, Martin H, Jolesz FA, Vykhodtseva N. The threshold for brain damage in rabbits induced by bursts of ultrasound in the presence of an ultrasound contrast agent (Optison). Ultrasound Med Biol. 2003; 29:473–481. [PubMed: 12706199]
34. Chen L, Wansapura JP, Heit G, Butts K. Study of laser ablation in the in vivo rabbit brain with MR thermometry. J Magn Reson Imaging. 2002; 16:147–152. [PubMed: 12203761]
35. McDannold N, Moss M, Killiany R, Rosene DL, King RL, Jolesz FA, Hynynen K. MRI-guided focused ultrasound surgery in the brain: Tests in a primate model. Magn Reson Med. 2003; 49:1188–1191. [PubMed: 12768598]
36. Cohen ZR, Zaubermann J, Harnof S, Mardor Y, Nass D, Zadicario E, Hananel A, Castel D, Faibel M, Ram Z. Magnetic resonance imaging-guided focused ultrasound for thermal ablation in the brain: A feasibility study in a swine model. Neurosurgery. 2007; 60:593–600. discussion. [PubMed: 17415195]
37. Aktas C, Kanter M. A morphological study on Leydig cells of scrotal hyperthermia applied rats in short-term. J Mol Histol. 2009; 40:31–39. [PubMed: 19184471]
38. Kanter M, Aktas C. Effects of scrotal hyperthermia on Leydig cells in long-term: A histological, immunohistochemical and ultrastructural study in rats. J Mol Histol. 2009; 40(2):123–30. [PubMed: 19484498]
39. Paul C, Murray AA, Spears N, Saunders PT. A single, mild, transient scrotal heat stress causes DNA damage, subfertility and impairs formation of blastocysts in mice. Reproduction. 2008; 136:73–84. [PubMed: 18390691]
40. Wang C, Cui YG, Wang XH, Jia Y, Sinha Hikim A, Lue YH, Tong JS, Qian LX, Sha JH, Zhou ZM, Hull L, Leung A, Swerdloff RS. Transient scrotal hyperthermia and levonorgestrel enhance testosterone-induced spermatogenesis suppression in men through increased germ cell apoptosis. J Clin Endocrinol Metab. 2007; 92:3292–3304. [PubMed: 17504903]

41. Luo Q, Li Z, Huang X, Yan J, Zhang S, Cai YZ. Lycium barbarum polysaccharides: Protective effects against heatinduced damage of rat testes and H2O2-induced DNA damage in mouse testicular cells and beneficial effect on sexual behavior and reproductive function of hemicastrated rats. Life Sci. 2006; 79:613–621. [PubMed: 16563441]
42. Banks S, King SA, Irvine DS, Saunders PT. Impact of a mild scrotal heat stress on DNA integrity in murine spermatozoa. Reproduction. 2005; 129:505–514. [PubMed: 15798026]
43. Paul C, Teng S, Saunders PT. A single, mild, transient scrotal heat stress causes hypoxia and oxidative stress in mouse testes, which induces germ cell death. Biol Reprod. 2009; 80:913–919. [PubMed: 19144962]
44. Perez-Crespo M, Pintado B, Gutierrez-Adan A. Scrotal heat stress effects on sperm viability, sperm DNA integrity, and the offspring sex ratio in mice. Mol Reprod Dev. 2008; 75:40–47. [PubMed: 17474098]
45. Lue Y, Wang C, Liu YX, Hikim AP, Zhang XS, Ng CM, Hu ZY, Li YC, Leung A, Swerdloff RS. Transient testicular warming enhances the suppressive effect of testosterone on spermatogenesis in adult cynomolgus monkeys (Macaca fascicularis). J Clin Endocrinol Metab. 2006; 91:539–545. [PubMed: 16317056]
46. Lue YH, Lasley BL, Laughlin LS, Swerdloff RS, Hikim AP, Leung A, Overstreet JW, Wang C. Mild testicular hyperthermia induces profound transitional spermatogenic suppression through increased germ cell apoptosis in adult cynomolgus monkeys (Macaca fascicularis). J Androl. 2002; 23:799–805. [PubMed: 12399525]
47. Seror O, Lepetit-Coiffe M, Le Bail B, de Senneville BD, Trillaud H, Moonen C, Quesson B. Real time monitoring of radiofrequency ablation based on MR thermometry and thermal dose in the pig liver in vivo. Eur Radiol. 2008; 18:408–416. [PubMed: 17899103]
48. Anderson CD, Lin WC, Beckham J, Mahadevan-Jansen A, Buttemere CR, Pierce J, Nicoud IB, Wright Pinson C, Chari RS. Fluorescence spectroscopy accurately detects irreversible cell damage during hepatic radiofrequency ablation. Surgery. 2004; 136:524–531. [PubMed: 15349097]
49. Lepetit-Coiffe M, Quesson B, Seror O, Dumont E, Le Bail B, Moonen CT, Trillaud H. Real-time monitoring of radiofrequency ablation of rabbit liver by respiratory-gated quantitative temperature MRI. J Magn Reson Imaging. 2006; 24:152–159. [PubMed: 16767739]
50. Kopelman D, Inbar Y, Hanannel A, Freundlich D, Castel D, Perel A, Greenfeld A, Salamon T, Sareli M, Valeanu A, Papa M. Magnetic resonance-guided focused ultrasound surgery (MRgFUS): Ablation of liver tissue in a porcine model. Eur J Radiol. 2006; 59:157–162. [PubMed: 16725294]
51. Zderic V, Foley J, Luo W, Vaezy S. Prevention of post-focal thermal damage by formation of bubbles at the focus during high intensity focused ultrasound therapy. Med Phys. 2008; 35:4292–4299. [PubMed: 18975674]
52. Hemmila MR, Foley DS, Casetti AV, Soldes OS, Hirschl RB, Bartlett RH. Perfusion induced hyperthermia for oncologic therapy with cardiac and cerebral protection. ASAIO J. 2002; 48:350–354. [PubMed: 12141462]
53. Haveman J, Smals OA, Rodermond HM. Effects of hyperthermia on the rat bladder: A pre-clinical study on thermometry and functional damage after treatment. Int J Hyperthermia. 2003; 19:45–57. [PubMed: 12519711]
54. Greenhalgh DG, Lawless MB, Chew BB, Crone WA, Fein ME, Palmieri TL. Temperature threshold for burn injury: An oximeter safety study. J Burn Care Rehabil. 2004; 25:411–415. [PubMed: 15353932]
55. Werner MU, Lassen B, Pedersen JL, Kehlet H. Local cooling does not prevent hyperalgesia following burn injury in humans. Pain. 2002; 98:297–303. [PubMed: 12127031]
56. Landsberg R, DeRowe A, Katzir A, Shtabsky A, Fliss DM, Gil Z. Laser-induced hyperthermia for treatment of granulation tissue growth in rats. Otolaryngol Head Neck Surg. 2009; 140:480–486. [PubMed: 19328334]
57. Ichinoseki-Sekine N, Naito H, Saga N, Ogura Y, Shiraishi M, Giombini A, Giovannini V, Katamoto S. Changes in muscle temperature induced by 434 MHz microwave hyperthermia. Br J Sports Med. 2007; 41:425–429. [PubMed: 17261552]
58. Rabkin BA, Zderic V, Crum LA, Vaezy S. Biological and physical mechanisms of HIFU-induced hyperecho in ultrasound images. Ultrasound Med Biol. 2006; 32:1721–1729. [PubMed: 17112958]

59. Sokka SD, King R, Hynynen K. MRI-guided gas bubble enhanced ultrasound heating in in vivo rabbit thigh. Phys Med Biol. 2003; 48:223–241. [PubMed: 12587906]
60. Mougenot C, Quesson B, de Senneville BD, de Oliveira PL, Sprinkhuizen S, Palussiere J, Grenier N, Moonen CT. Threedimensional spatial and temporal temperature control with MR thermometry-guided focused ultrasound (MRgHIFU). Magn Reson Med. 2009; 61:603–614. [PubMed: 19097249]
61. Nosaka K, Muthalib M, Lavender A, Laursen PB. Attenuation of muscle damage by preconditioning with muscle hyperthermia 1-day prior to eccentric exercise. Eur J Appl Physiol. 2007; 99:183–192. [PubMed: 17089155]
62. Morrison SA, Sleivert GG, Cheung S. Aerobic influence on neuromuscular function and tolerance during passive hyperthermia. Med Sci Sports Exerc. 2006; 38:1754–1761. [PubMed: 17019297]
63. He X, McGee S, Coad JE, Schmidlin F, Iaizzo PA, Swanlund DJ, Kluge S, Rudie E, Bischof JC. Investigation of the thermal and tissue injury behaviour in microwave thermal therapy using a porcine kidney model. Int J Hyperthermia. 2004; 20:567–593. [PubMed: 15370815]
64. Nakada SY, Jerde TJ, Warner TF, Wright AS, Haemmerich D, Mahvi DM, Lee FT Jr. Bipolar radiofrequency ablation of the kidney: Comparison with monopolar radiofrequency ablation. J Endourol. 2003; 17:927–933. [PubMed: 14744366]
65. Ogan K, Roberts WW, Wilhelm DM, Bonnell L, Leiner D, Lindberg G, Kavoussi LR, Cadeddu JA. Infrared thermography and thermocouple mapping of radiofrequency renal ablation to assess treatment adequacy and ablation margins. Urology. 2003; 62:146–151. [PubMed: 12837456]
66. Lee JM, Han JK, Choi SH, Kim SH, Lee JY, Shin KS, Han CJ, Choi BI. Comparison of renal ablation with monopolar radiofrequency and hypertonic-saline-augmented bipolar radiofrequency: In vitro and in vivo experimental studies. Am J Roentgenol. 2005; 184:897–905. [PubMed: 15728615]
67. Diederich, CJ.; Nau, WH.; Kinsey, A.; Ross, T.; Wootton, J.; Juang, T.; Butts-Pauly, K.; Rieke, V.; Chen, J.; Bouley, DM.; Sommer, G. Catheter-based ultrasound devices and MR thermal monitoring for conformal prostate thermal therapy; Conf Proc IEEE Eng Med Biol Soc, Vancouver, BC 20-25 Aug. 2008; 2008. p. 3664-3668.
68. Nau WH, Diederich CJ, Ross AB, Butts K, Rieke V, Bouley DM, Gill H, Daniel B, Sommer G. MRI-guided interstitial ultrasound thermal therapy of the prostate: A feasibility study in the canine model. Med Phys. 2005; 32:733–743. [PubMed: 15839345]
69. Ross AB, Diederich CJ, Nau WH, Rieke V, Butts RK, Sommer G, Gill H, Bouley DM. Curvilinear transurethral ultrasound applicator for selective prostate thermal therapy. Med Phys. 2005; 32:1555–1565. [PubMed: 16013714]
70. Pauly KB, Diederich CJ, Rieke V, Bouley D, Chen J, Nau WH, Ross AB, Kinsey AM, Sommer G. Magnetic resonance-guided high-intensity ultrasound ablation of the prostate. Top Magn Reson Imaging. 2006; 17:195–207. [PubMed: 17414077]
71. Chopra R, Tang K, Burtnyk M, Boyes A, Sugar L, Appu S, Klotz L, Bronskill M. Analysis of the spatial and temporal accuracy of heating in the prostate gland using transurethral ultrasound therapy and active MR temperature feedback. Phys Med Biol. 2009; 54:2615–2633. [PubMed: 19351975]
72. Kinsey AM, Diederich CJ, Rieke V, Nau WH, Pauly KB, Bouley D, Sommer G. Transurethral ultrasound applicators with dynamic multi-sector control for prostate thermal therapy: In vivo evaluation under MR guidance. Med Phys. 2008; 35:2081–2093. [PubMed: 18561684]
73. Mencucci R, Ambrosini S, Ponchietti C, Marini M, Vannelli GB, Menchini U. Ultrasound thermal damage to rabbit corneas after simulated phacoemulsification. J Cataract Refract Surg. 2005; 31:2180–2186. [PubMed: 16412936]
74. Takahashi Y, Igaki M, Suzuki A, Takahashi G, Dogru M, Tsubota K. The effect of periocular warming on accommodation. Ophthalmology. 2005; 112:1113–1118. [PubMed: 15885788]
75. Kandulla J, Elsner H, Birngruber R, Brinkmann R. Noninvasive optoacoustic online retinal temperature determination during continuous-wave laser irradiation. J Biomed Optics. 2006; 11:041111.

76. Blackie CA, Solomon JD, Greiner JV, Holmes M, Korb DR. Inner eyelid surface temperature as a function of warm compress methodology. Optom Vis Sci. 2008; 85:675–683. [PubMed: 18677234]

77. Melodelima D, Salomir R, Chapelon JY, Theillere Y, Moonen C, Cathignol D. Intraluminal high intensity ultrasound treatment in the esophagus under fast MR temperature mapping: In vivo studies. Magn Reson Med. 2005; 54:975–982. [PubMed: 16155893]

78. Lambert GP, Gisolfi CV, Berg DJ, Moseley PL, Oberley LW, Kregel KC. Selected contribution: Hyperthermia-induced intestinal permeability and the role of oxidative and nitrosative stress. J Appl Physiol. 2002; 92:1750–1761. discussion 49. [PubMed: 11896046]

79. Sugiura M, Kuwabara Y, Mitani M, Sato A, Shinoda N, Kimura M, Yano M, Mitsui A, Suzuki T, Fujii Y. Effect of whole body hyperthermia on ischemia and reperfusion injury of rat intestine: Real-time ATP change studied using P-31- MRS. Eur Surg Res. 2002; 34:306–312. [PubMed: 12145557]

80. Eriksson AR, Albrektsson T. Temperature threshold levels for heat-induced bone tissue injury: A vital-microscopic study in the rabbit. J Prosthetic Dentistry. 1983; 50:101–107.

81. Alvarado R, Mahon B, Valadez C, Caufield M, Wadhwani S, Hambleton C, Siziopikou KP, Dickler AT, Gatta J, Dowlatshahi K. Thermal ablation of the goat mammary gland as a model for post-lumpectomy treatment of breast cancer: Preliminary observations. Int J Hyperthermia. 2009; 25:47–55. [PubMed: 19219700]

82. Yoshida N, Kristiansen A, Liberman MC. Heat stress and protection from permanent acoustic injury in mice. J Neurosci. 1999; 19:10116–10124. [PubMed: 10559419]

83. Murakoshi M, Yoshida N, Kitsunai Y, Iida K, Kumano S, Suzuki T, Kobayashi T, Wada H. Effects of heat stress on Young's modulus of outer hair cells in mice. Brain research. 2006; 1107:121–130. [PubMed: 16822487]

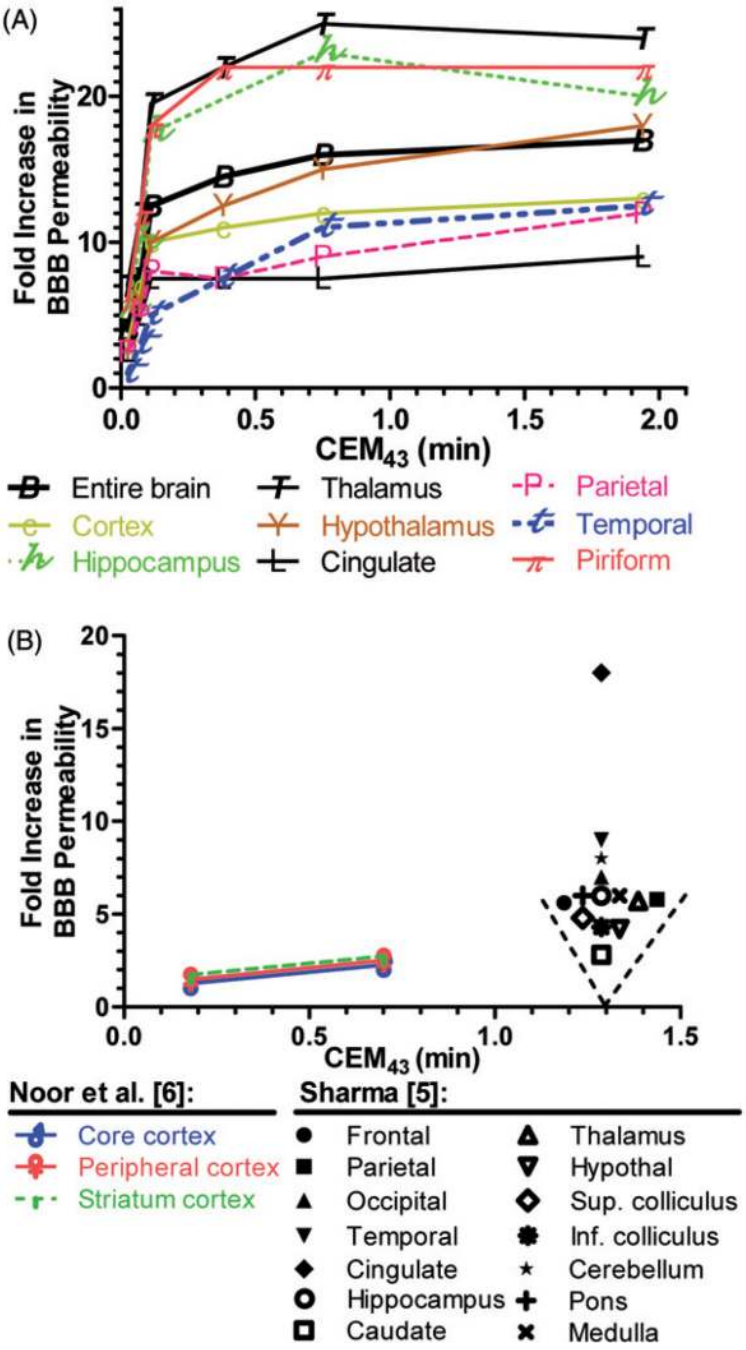

Fig 1.

Changes in regional blood brain barrier permeability vs. CEM_{43} after hyperthermia treatment in rats. (A) Fold increase in BBB permeability immediately after whole body heating with a warming pad by Kiyatkin et al. [4]. (B) Increase in BBB permeability immediately following heating in an incubator to CEM_{43}=1.3 min by Sharma [5] and 24 h following heating on a warming pad to CEM_{43}=0.1–0.7 min by Noor et al. [6]. In (B), some of the data was offset along the *x*-axis to show all the data points clearly. All data bound by the dashed lines refer to CEM_{43}=1.3 min.

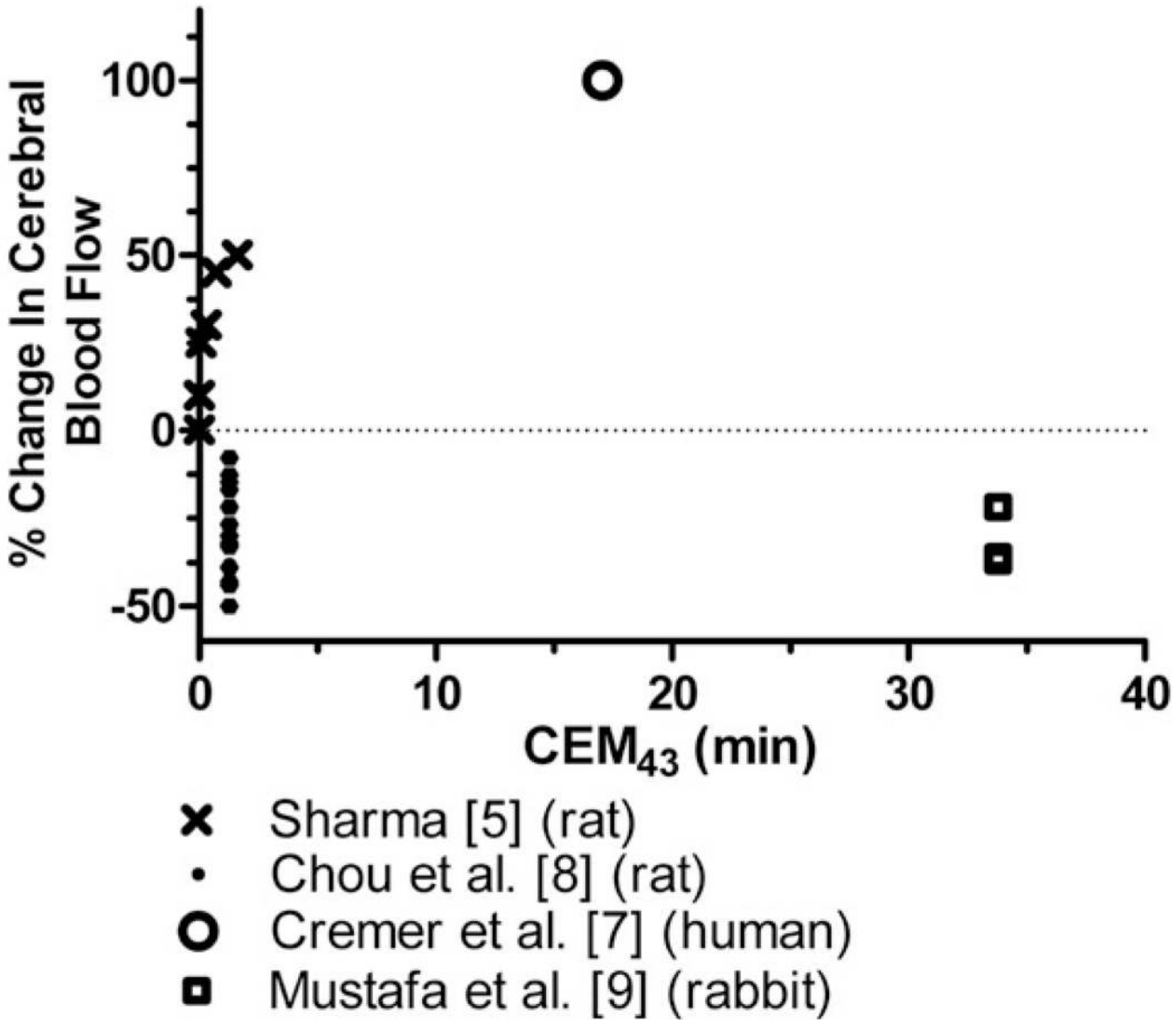

Fig 2.

Change in cerebral blood flow vs. CEM_{43}. Measurements were made either during or immediately after whole body hyperthermia treatment in rats, humans, and rabbits [5, 7–9].

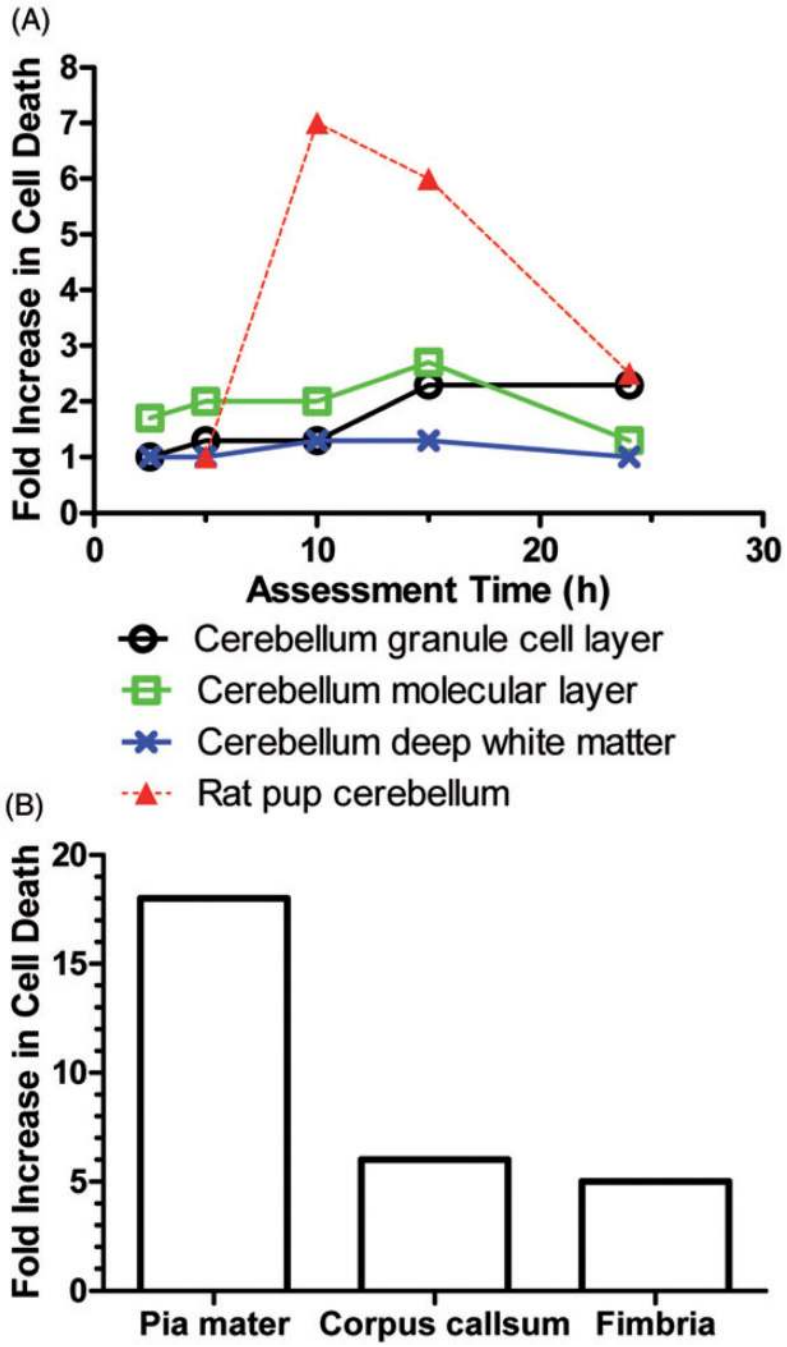

Fig 3.

Heat-induced cell death in the rat brain. (A) Cell death in several brain regions at multiple assessment times after whole body hyperthermia treatment in rats at CEM_{43}=5.9 min [10]. (B) Fold increase in cell death in several brain regions in rats compared to unheated animals, 10 hours after whole body hyperthermia treatment to CEM_{43}=15 min [11].

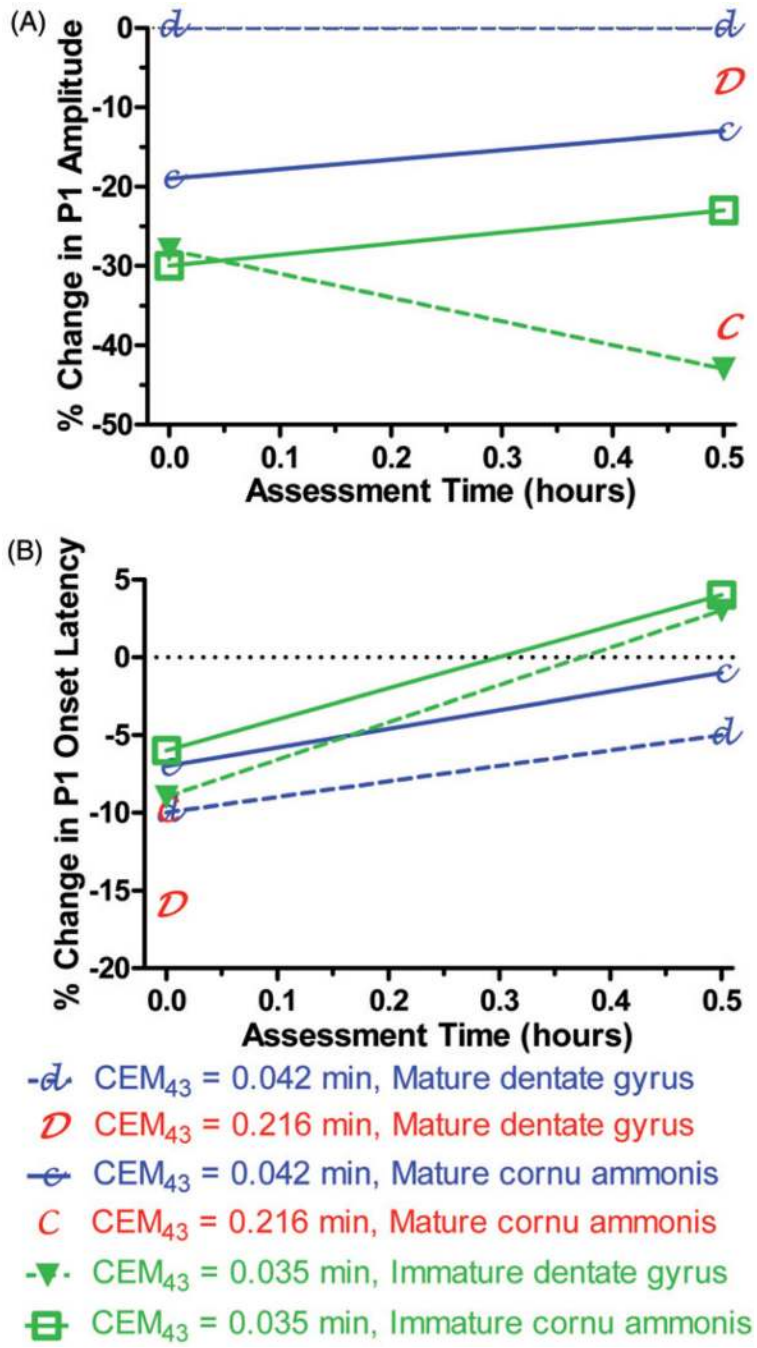

Fig 4.

Changes in neuronal excitability in two regions of hippocampus following whole body hyperthermia in rats (immediately and 30 min after heating). Data are shown as percent change with respect to baseline measurements (data connected by lines where assessed at both time points). Two different CEM_{43} are plotted for the mature rats. (A) P1 Amplitude, (B) P1 Onset Latency [15].

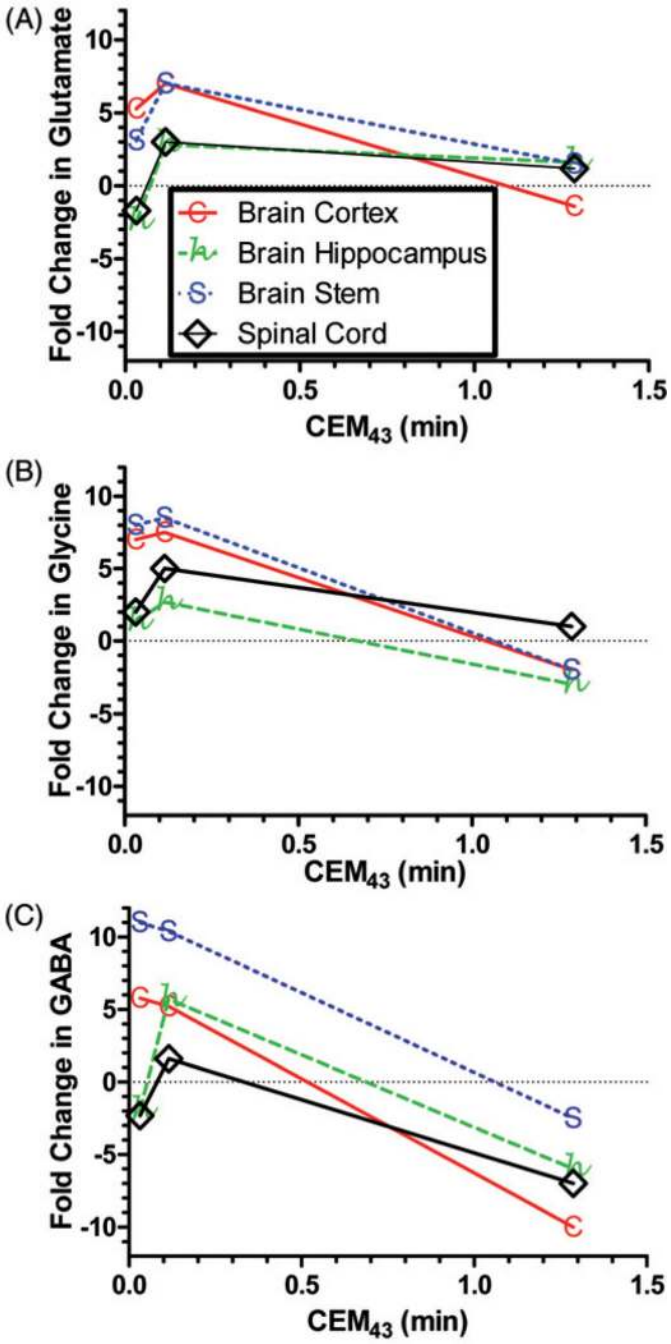

Fig 5.

Heat-induced neurotransmitter concentration changes in the rat brain. (A) glutamate, (B) glycine, and (C) GABA levels are shown in relation to CEM_{43} in various rat brain regions immediately following whole body hyperthermia [5].

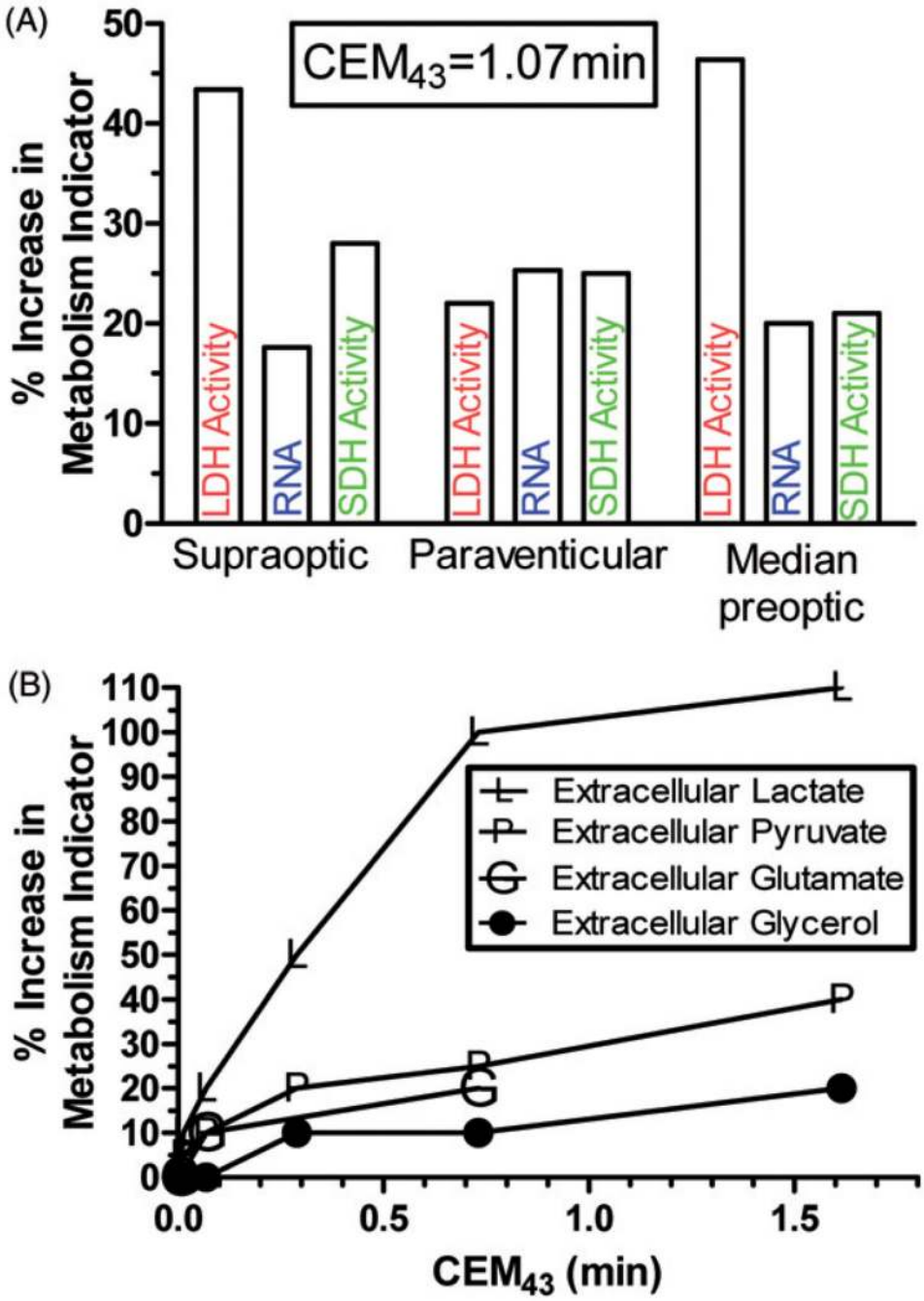

Fig 6.

Changes in rat brain metabolism immediately after whole body hyperthermia. (A) Metabolic changes were assessed by lactate dehydrogenase (LDH) and succinate dehydrogenase (SDH) activity and RNA content at CEM_{43}=1.07 min in three rat brain regions [20], and (B) metabolic changes vs. CEM_{43}, as assessed by extracellular brain lactate, pyruvate, glutamate, and glycerol concentrations vs. CEM_{43} [8].

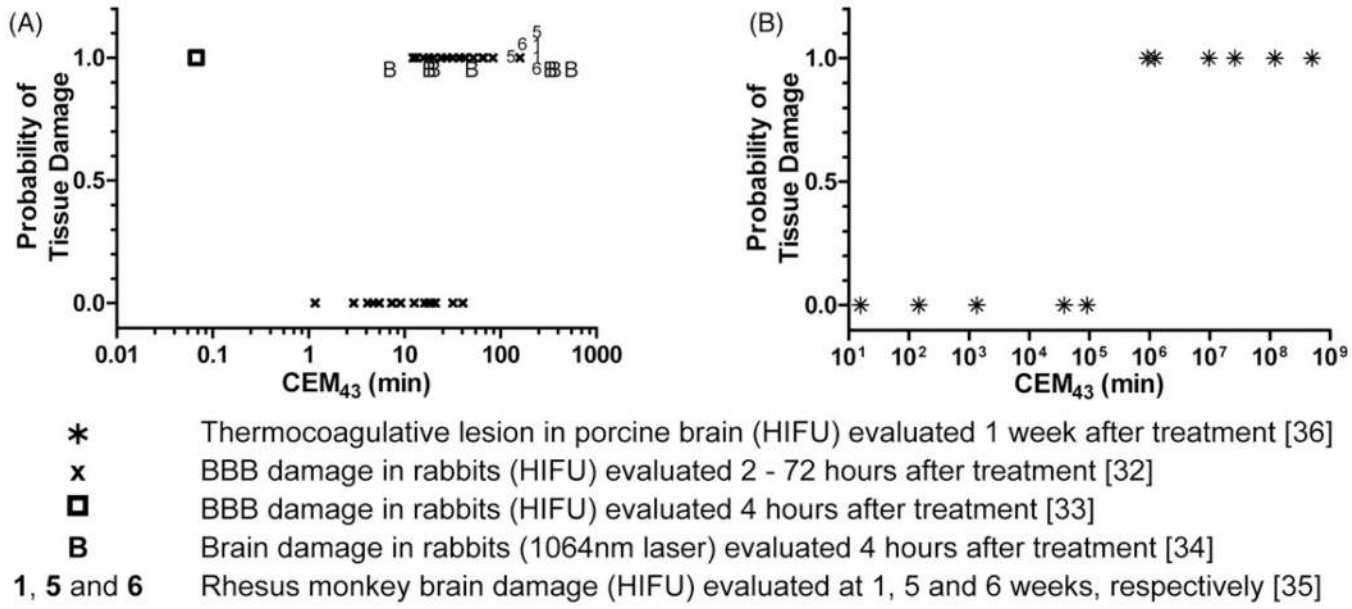

Fig 7.

Probability of brain lesion induction and blood brain barrier disruption vs. CEM_{43} in (A) rabbits and rhesus monkeys and (B) pigs [32–36]. In (A), some of the data were offset along the *y*-axis to show all the data points above CEM_{43}=100 min.

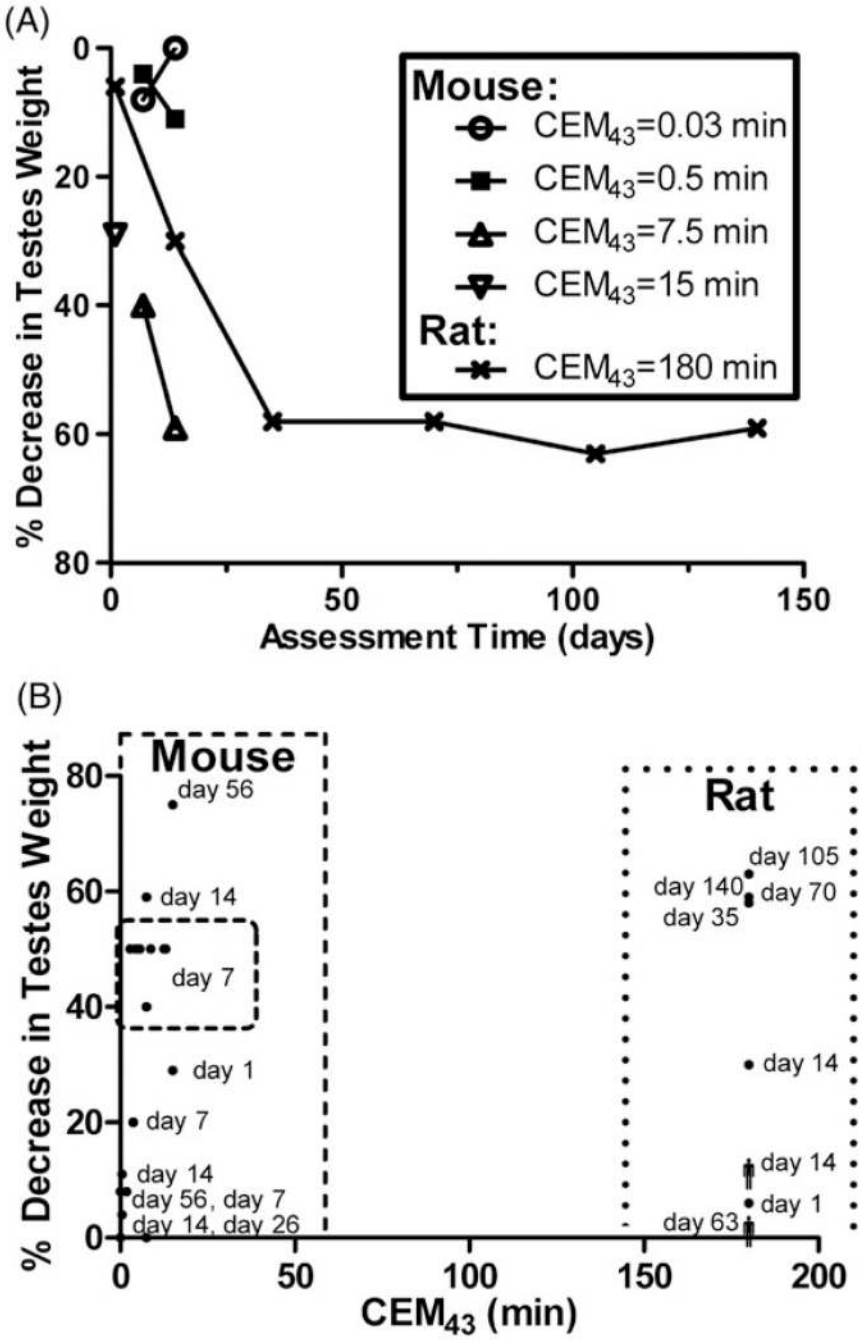

Fig 8.

Decrease in testes weight compared to control. (A) % Decrease in weight of tested vs. assessment time at several thermal doses. (B) Changes in testicular weight assessed at various times, grouped by CEM_{43}. Human data are included for comparative purposes, but human data was reported as a measure of % decrease in volumetric measures. This chart highlights the differences in thermal sensitivity between mouse, rat, and human testes (blue symbols) [37–41].

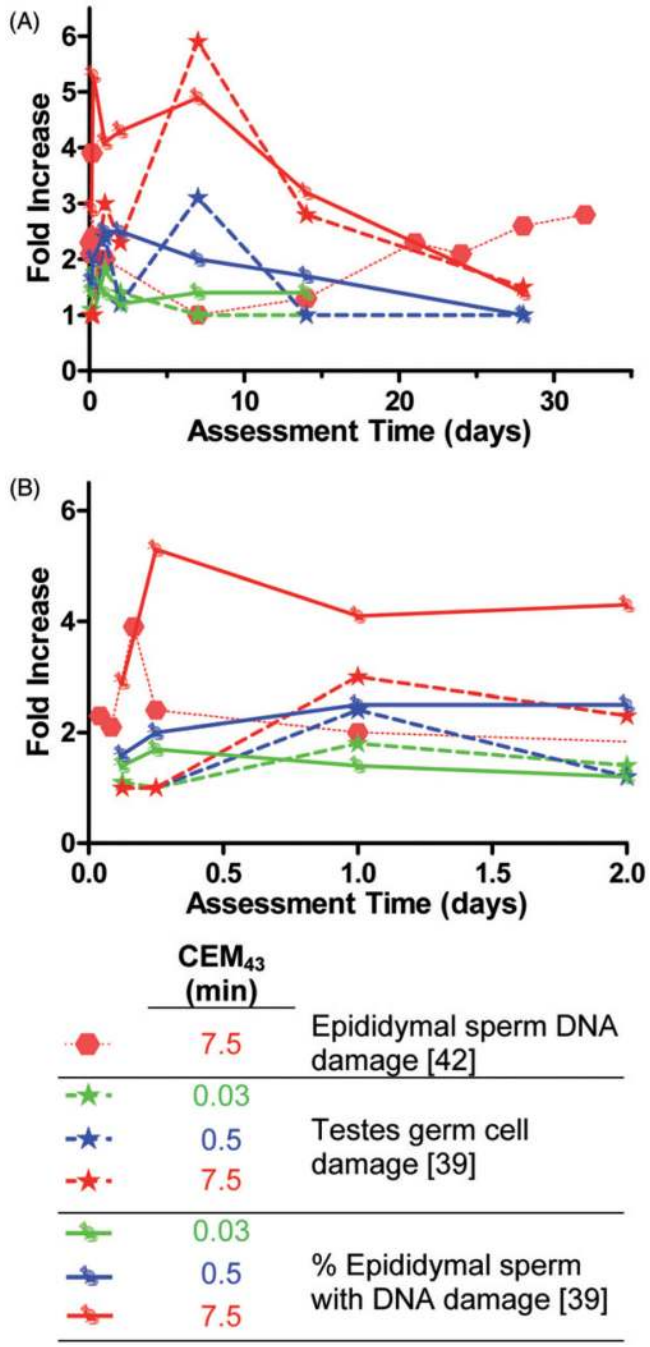

Fig 9.

Fold increase in cell damage parameters after various heat treatments in mice. (A) Long-term effects, which illustrate that cell damage increases with thermal dose and that the effects occur in two phases: an early and a late phase. (B) Acute cell damage during the first two days.

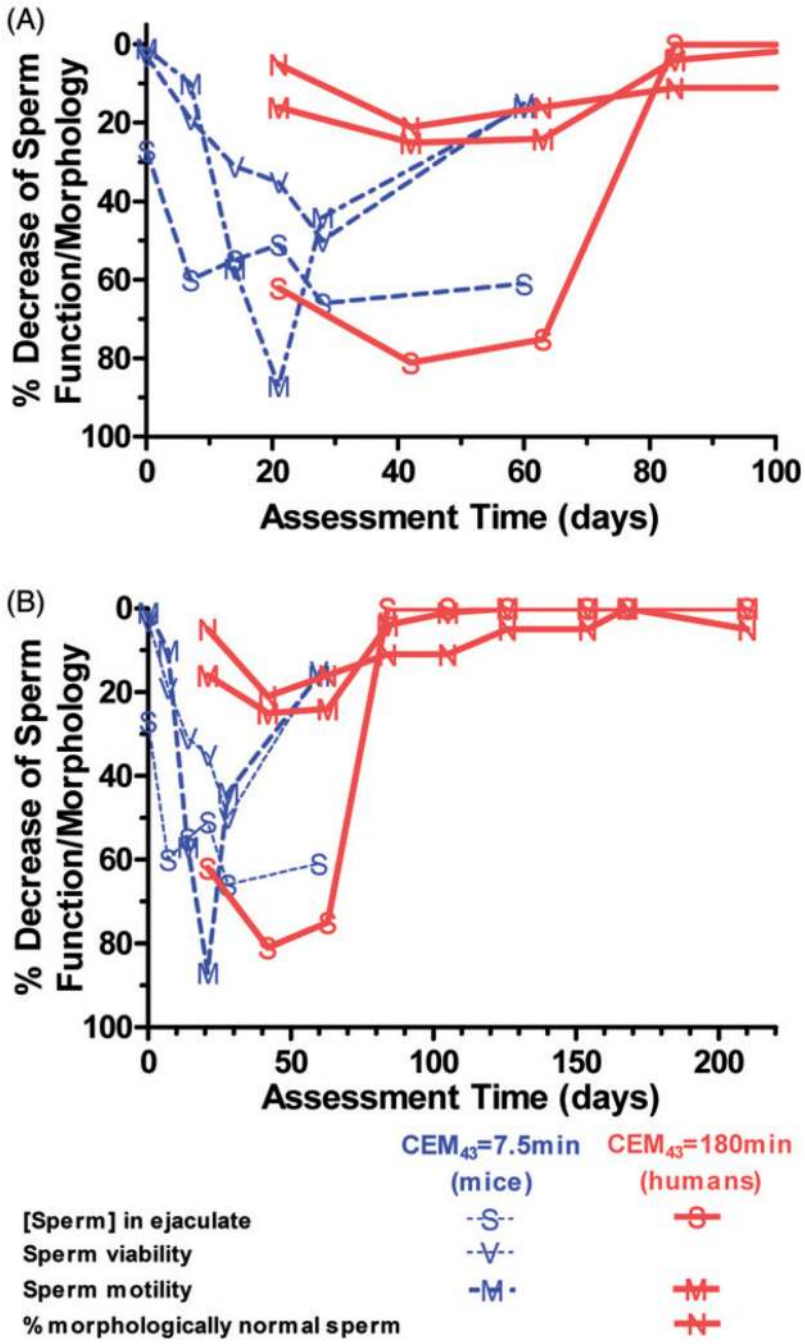

Fig 10.

Indications of sperm function after heating in mice and humans. (A) Early effects of heating on sperm characteristics. (B) Late effects of heating on sperm characteristics. Dashed lines: mouse data with a thermal dose of CEM_{43}=7.5 min [44]. Solid lines: human data with a thermal dose of CEM_{43}=180 min [40].

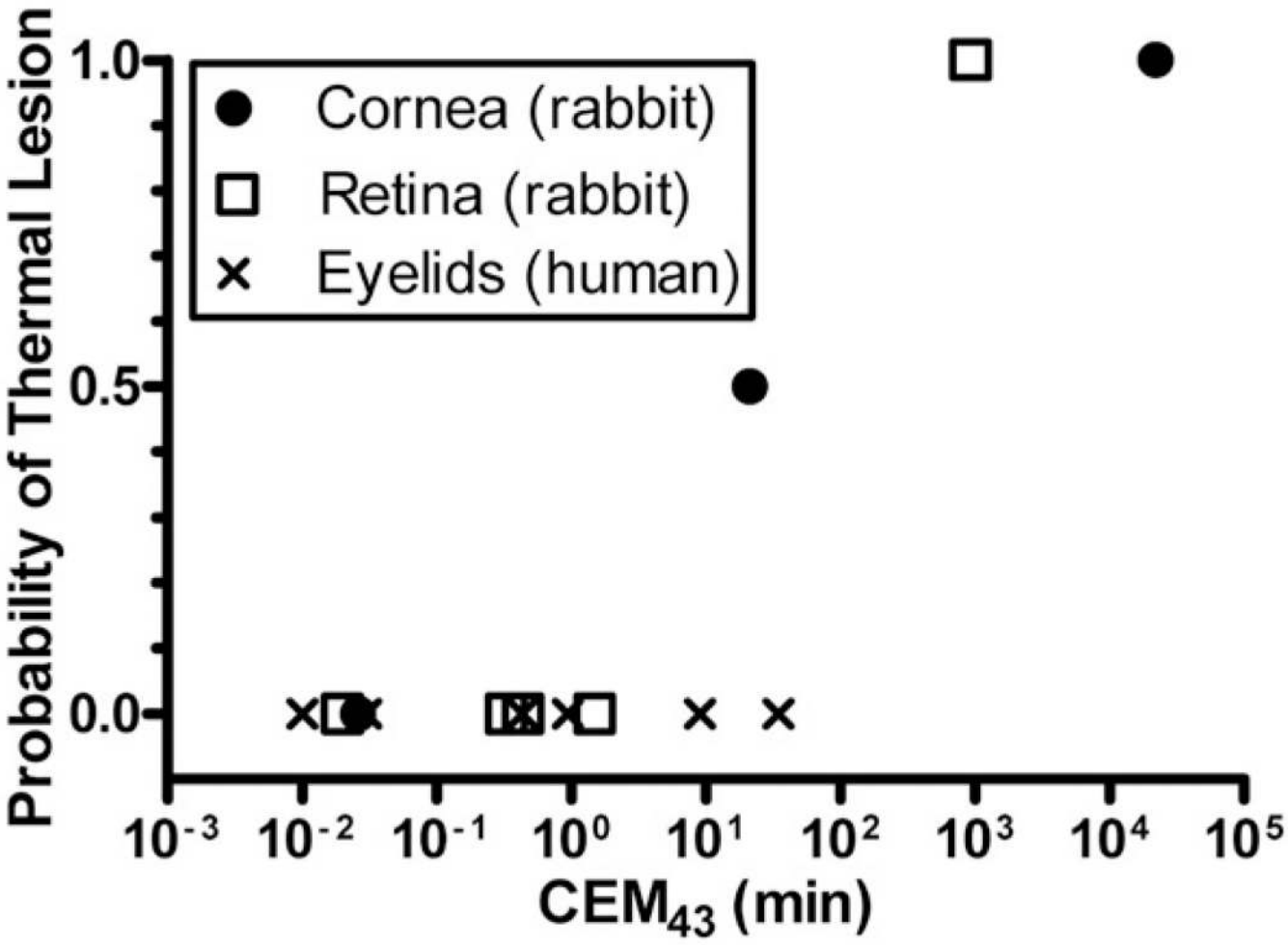

Fig 11.

Thresholds of thermal damage in eye in rabbits and humans assessed immediately after heating. In rabbits, CEM_{43}>21.3 min [73] started causing thermal damage in cornea while thermal lesion in retina was induced at CEM_{43}=926 min [75]. In humans, heat treatment at CEM_{43}=0.015–34.5 min was not sufficient to cause damage to eyelids [76].

Table I

Keywords used in database searches.

Hyperthermia damage	Laser burn	Skin
Heat damage	Heat	Tendon
High temperature damage	Soft tissue	Muscle
Heat exposure damage	Adipose	Epicardium
Hyperthermia injury	Tissue	Bone
Heat injury	Liver	Spine
High temperature injury	Oesophagus	Fat
Heat exposure injury	Intestine	Foot
High temperature tissue destruction	Testis/testes	Tail
High temperature tissue damage	Prostate	Spleen
Heat tissue destruction	Bladder	Bone marrow
Heat temperature tissue damage	Urethra	Brain
Heat inflammation	Kidney	Spinal cord
Heat exposure damage	Eye	Blood vessels
Heat exposure injury	Cornea	Gonads
CNS/Central Nervous	Retina	Ovaries/ovary
Blood–brain barrier	Lens	Gonads
Peripheral nerve system	Iris	Burn injury
	Eyelids	

Table II

Summary of thermal damage threshold data compiled in the earlier review updated with newer literature.

		Type and degree change					
		Acute		Chronic			
CEM_{43} (min)	Tissue type	Minor	Significant	Minor	Significant	Animal	Reference
0–20	BBB		H*/F, *H/F*			Rat/Rabbit, *Dog*	[4, 5, 32, 33]
	Bone				G	Rabbit	[80]
	Bone Marrow	*F/H*	H*			*Mouse*, Rat	[11]
	Brain	H/*H*	H	*H*		Rat/*Dog*, Rabbit, *Cat*	[4, 5, 10, 11, 34]
	Cornea		F			Human	[74]
	Esophagus		H			Pig	[77]
	Kidney	*H*	F			*Rabbit*, Rabbit	[9]
	Muscle		F*/H			Human/Pig	[58, 61]
	Retina			*G/H*		*Rabbit*	
	Testis	*F*, F/H	*H*, H/F/G	*F*, H	*F*, F	*Mouse*, Mouse	[39, 42–44]
	Testis		G, H*			Rat	[10, 41]
	Thymus		H*			Rat	[11]
	Small Intestine		F/H			Rat	[78]
	Nerve		F			Rat	[25, 29, 31]
21–40	BBB		H/*F*			Rabbit/*Dog*	[32]
	Brain	*H/G*	H	*H/G*		*Dog*, Rabbit	[34]
	Cornea	G/*G*				Rabbit/*Rabbit*	[73]
	Eyelid	*G*				*Rabbit*	
	Mammary Gland		H			Goat	[81]
	Prostate			*H*		*Dog*	
	Retina	*G*				*Rabbit*	
	Skin	*F*				*Mouse*	
	Small Intestine		*H*			*Mouse*	
41–80	Bladder		F↓			Rat	[53]
	Bone				G	Rabbit	[80]
	Brain		H*, *H/G*		*H/G*	Rabbit, *Dog*	[34]
	Cornea		*G*			*Rabbit*	
	Kidney		H			Pig	[63]
	Liver	F ↑*/*H*				Dog/*Rabbit*	[52]
	Muscle	*H*				*Pig*	
	Prostate	*H*	*G*			*Dog*	
	Retina		*G*	*G*		*Rabbit*	
	Skin		*G/H*		*G/H*	*Mouse*	
	Testis		H/F↓		F	Monkey	[45]
	BBB		H			Rabbit	[32]
80–240	Bladder		F ↓		*G*	Rat, *Dog*	[53]
	Bone				G	Rabbit	[80]
	Eyelid	*G*				*Rabbit*	
	Muscle		H	*G/H*	*G/H*	Rat, *Pig*	[56]
	Skin		*G/H*		*G*	*Pig*	
	Small Intestine		*H*		*G/H*	*Pig/Dog*	
	Testis		G/F		G/F	Rat	[37, 38]
	Testis		F↓	F		Monkey	[46]
	Testis	H/F	H/F↓	F		Human	[40]
	Brain		H		*H*	Monkey	[35]
	BBB		H			Rabbit	[32]
>240	Cornea		G			Rabbit	[73]
	Esophagus		G			Pig	[77]
	Kidney		H			Pig/Dog	[63–66]
	Liver		H			Rabbit/Pig	[47–49, 51]
	Muscle		H/G			Rabbit/Pig	[51, 59, 60]
	Prostate		H			Dog	[67–70, 72]
	Retina		G/*G*			Rabbit/ *Rabbit*	[75]
	Skin		H			Human	[54]
	Brain		H/G		H	Rabbit/Pig/Monkey	[34–36]

Bold, black: new data, Bold, underlined, red: new organs not covered in the previous review, *Italicized, blue: data from Table 3 in [1] (reference numbers are not stated in the table)*. Acute (Tissue evaluated 0–30 days after heat exposure); Chronic (Tissue evaluated >30 days after heat exposure). Damage quantification: Histolopathology (H); Gross appearance (G); Function (F).

BBB - blood brain barrier.

Eyelid study showed no damage up to CEM_{43} = 9.08 min.

Bladder function (volume) showed the opposite trend at different CEM_{43}.

Ultrasound heating caused tissue damage in cornea at CEM_{43} as low as 2.7 min, whereas diode laser heating did not show any damage at CEM_{43} up to 1.26×10^{3} min.

* signifies whole body heat treatment.

Table III

Changes in testicular tubule dimensions in human subjects heated with CEM_{43}=180 min.

Evaluation time point post-treatment	% Change in tubule diameter	% Change in tubule	% Change in lumen volume
2 weeks	−10%	−3%	−3%
9 weeks	+2%	+6%	−11%